INTERFEROMETRIC MEASUREMENT OF FREE CONVECTION HEAT TRANSFER COEFFICIENTS IN THE TRANSITIONAL AND TURBULENT REGIMES

A THESIS

Presented to

The Faculty of the Division of Graduate

Studies and Research

By

Jack K. Norris II

In Partial Fulfillment

of the Requirements for the Degree

Master of Science in Mechanical Engineering

Georgia Institute of Technology

August, 1973

INTERFEROMETRIC MEASUREMENT OF FREE CONVECTION HEAT TRANSFER COEFFICIENTS IN THE TRANSITIONAL AND TURBULENT REGIMES

Approved:

William Z. Black, Chairman

S. P. Kezios

E. W. Thomas

Date approved by Chairman: 8/22/23

ACKNOWLEDGEMENTS

I would like to thank all those who assisted in the completion of this investigation. My special thanks to Dr. W. Z. Black, who suggested the problem and who gave freely of this time, advice, and patience. Also, I would like to thank T. E. Clopton for his technical assistance in constructing the associated electrical equipment and to D. Cabe for his assistance and advice in the building of the experimental apparatus.

Finally, I wish to extend my deepest gratitude to the U. S. Army for permitting me to further my education and for giving the financial support to do so.

TABLE OF CONTENTS

TABLE OF CONTENTS (Continued)

LIST OF TABLES

LIST OF ILLUSTRATIONS

NOMENCLATURE

Symbol	Definition	Units
g	distance between WP1 and spherical mirror	ft.
G	Gladstone - Dale coefficient	ft^3/lb_m
Gr	Grashof number	dimensionless
h	local heat transfer coefficient	$Btu/hr\text{-}ft^2{}^\circ R$
k_r	thermal conductivity of air at T_r	$Btu/hr\text{-}ft^\circ R$
k_s	thermal conductivity of air at T_s	$Btu/hr\text{-}ft^\circ R$
L	width of plate	ft.
M	number of fringe shifts	dimensionless
Δn	difference between the extraordinary and ordinary index of refraction of birefringent material	dimensionless
Nu_x	local Nusselt number	dimensionless
P	absolute atmospheric pressure	lb_f/ft^2
Pr	Prandtl number	dimensionless
Ra_x	local Rayleigh number ($Pr\ Gr_x$)	dimensionless
T_a	ambient air temperature	$^\circ R$
T_r	reference temperature	$^\circ R$
T_s	plate surface temperature	$^\circ R$
x	distance from leading edge	ft.
α	angle of plate inclination	degrees
θ	wedge angle of Wollaston prism	radians
λ	wave lengthoof light	ft.

SUMMARY

This thesis describes the application of the differential interferometer to the measurement of local heat transfer coefficient in the transitional and turbulent regime of natural convection. The objective of this investigation was to determine the applicability of the differential interferometer to measurement of local heat transfer coefficients in the turbulent and transitional regimes. This objective was accomplished by measuring local heat transfer coefficients in the transitional and turbulent regimes of natural convection from an upward facing isothermally heated highly inclined plate.

Heat transfer rates were determined by placing an isothermally heated inclined plate in the viewing section of a differential interferometer. Motion pictures of the fringe deflections caused by the heated air were used for local instantaneous heat flux measurements and flow visualization studies. These motion pictures provided a sequence of instantaneous parallel fringe deflections which could be related to the instantaneous local heat transfer coefficient. The local heat transfer coefficient was determined by time averaging the local instantaneous heat transfer coefficients. Infinite fringe pattern photos were used to observe variation in the boundary layer to determine the approximate location of onset of transition and turbulence and to observe oscillations in the flow of heated air.

Four tests were conducted, one each at 45°, 60°, 70°, and 80°

inclinations from the vertical. All tests were conducted in air at Rayleigh numbers from 3×10^5 to 9.5×10^9.

The primary conclusions of this investigation are as follows: the differential interferometer can be used to measure local heat transfer coefficients in the transitional and turbulent flow regimes of natural convection; the interferometer also provides fringe patterns that are an excellent means of observing the flow structure within the thermal boundary layers; heat transfer coefficients measured by the differential interferometer in the turbulent flow regime above an isothermal inclined plate are in good agreement with previously published results; and heat transfer coefficients in the fully turbulent regime of an inclined plate are not dependent on angle of inclination or length from leading edge.

CHAPTER I

INTRODUCTION

Interferometers have been extensively employed in the study of heat transfer because they possess several distinct advantages over other measuring devices. The major advantages are that the presence of a light ray does not disturb the flow as would a thermocouple, hot wire anemometer, or other such device. Likewise, there is little inertia associated with a light ray; this promotes instantaneous response to rapidly changing conditions. Lastly, these devices are excellent in providing a visualization of the flow field because they graphically display the thermal boundary layer and types of flow regimes that surround a heated object.

Two of the most prominent men to employ the Mach Zehnder interferometer to flow visualization are ERG Eckert and B. Gebhart. ERG Eckert made extensive studies of natural convection from vertical plates [11, 13] and many textbooks, for example that of Krieth [32], display pictures of his interferograms depicting the laminar, transitional, and turbulent flow regimes. Gebhart, on the other hand, used the interferometer in stability studies of natural convection from vertical surfaces as treated in his article "Natural Convection Flow, Instability and Transition" [17].

The Mach Zehnder interferometer, the type of interferometer used by Eckert and Gebhart, has been the most widely employed inter-

ferometer in heat transfer studies. The Mach Zehnder interferogram produces fringe lines that are identical to isotherms. The measurement of heat transfer coefficients requires approximating the temperature gradient by knowing the precise location of the isotherms. This need to accurately locate isotherms and then approximate gradients has made the problem of determining heat transfer coefficients in all but laminar flow extremely difficult. Eckert and Soehnghen [13] stated that these fringe lines fluctuate quite rapidly throughout the boundary layer even at the solid surface and are not clearly visible in photographs taken from the flow, however, they can be seen with the aid of a magnifying glass.

To illustrate the difficulty in measuring the heat transfer coefficients in turbulent flow with a Mach Zehnder interferometer, the variation in air temperature a small distance away from an isothermal plate was calculated. Details of these calculations are presented in Appendix A. The parallel fringe pattern produced by a differential interferometer was used to calculate the air temperature 3.51×10^{-3} feet normal to a 282°F isothermal plate. The air temperature varied from a low temperature of 251°F to a high of 260°F during a five second interval (Figure 1a). This temperature variation caused a Mach Zehnder fringe shift between 27 and 30 fringes (Figure 1b). Due to the large number of fringe shifts produced, visualization of the instantaneous temperature necessary for prediction of the local heat transfer coefficient is extremely difficult with a Mach Zehnder interferometer and as a result its application

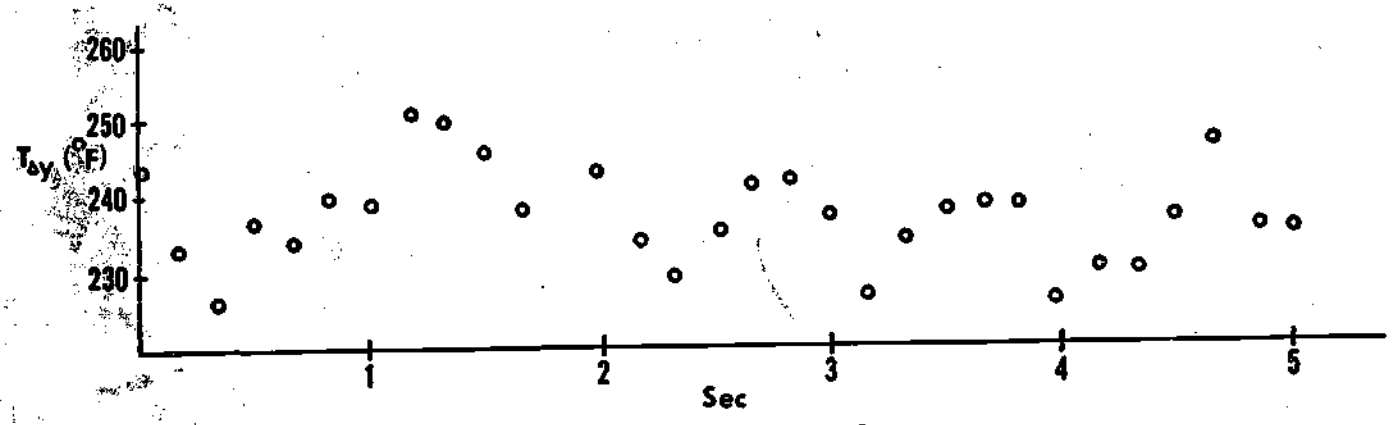

Figure 1a. Temperature Variation .351 x 10^{-2} feet Above 45° Inclined Plate Heated to Temperature of 282°F at Ra_x = 5.03 x 10^9.

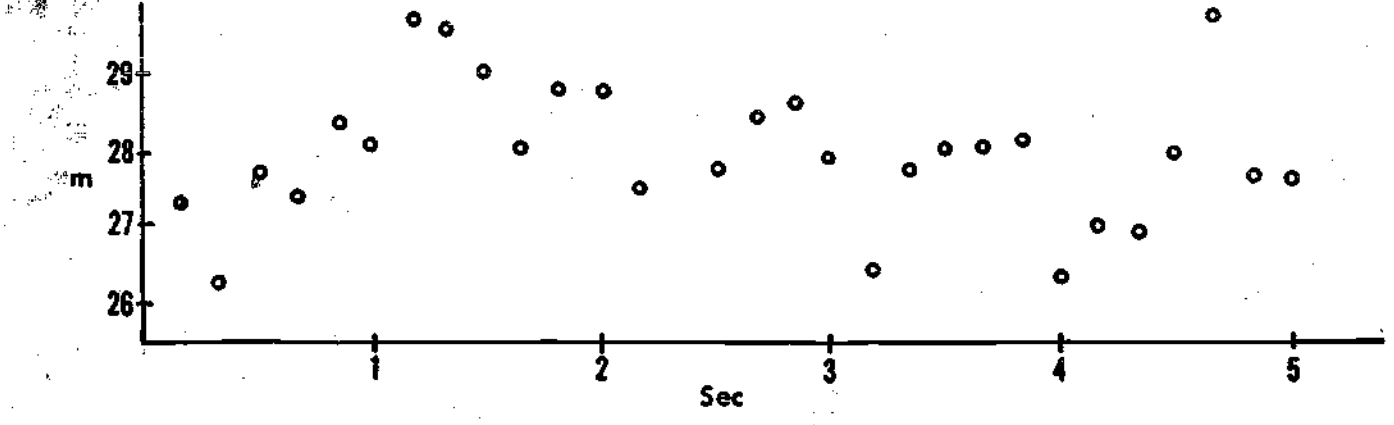

Figure 1b. Fringe Deflection, m, for a Mach Zehnder Interferometer for Temperature Variation in Figure 1a.

to heat transfer problems has been limited to measurements of heat transfer in the laminar flow regime or to flow visualizations.

Unlike the Mach Zehnder interferometer, the differential interferometer has not been widely used in heat transfer research. Its interferograms produce a parallel fringe pattern that can be directly related to temperature gradients. Therefore, by using this interferometer, it is not necessary to locate isotherms and approximate temperature gradients to determine heat transfer coefficients. The only measurement necessary is the relative displacement of an individual fringe line at the surface of the heated object. This relative fringe displacement is directly relatable to the heat transfer coefficient as will be discussed in more detail in Chapter III. The differential interferometer provides a much simpler procedure for the determination of heat transfer coefficients and because of this simplicity it was decided to attempt to measure free convection heat transfer coefficients in transitional and turbulent flow regimes.

In order to keep the experiment as simple as possible it was decided that free rather than forced convection would be used. This would greatly simplify construction of the test apparatus by eliminating the need for blowers and associated ductwork. Secondly, by inclining a flat plate from the verticle, the critical Rayleigh number marking the onset of transitional and turbulent flow could be reduced by an order of three or more magnitudes [51]. This meant that the flat plate would be shorter and lighter facilitating

construction and operation.

In conducting a literature survey of heat transfer work in the field of natural convection from inclined surfaces, it was found that little had been done in the transitional and turbulent regimes. (See Chapter II) Therefore, in concomitance with determining the applicability of using the interferometer in measuring heat transfer coefficients in natural convection a secondary objective was proposed. The differential interferometer was to be used in connection with an isothermal highly inclined flat plate to determine:

(1) Local Nusselt number in the transitional and turbulent flow regimes.

(2) Boundary layer thickness.

(3) Critical Rayleigh numbers marking the onset of transition and turbulent flow as a function of plate inclination.

CHAPTER II

LITERATURE SURVEY

A survey of literature dealing with natural convection from upward facing heated flat plates revealed that most natural convection studies have been conducted from vertical or horizontal flat plates, [1-4, 7, 9-15, 17-24, 27, 28, 32-34, 37-39, 43-45, 47, 48, 52-54], and one quickly agrees with C. G. Vliet's introductory statement: "Transitional and turbulent data for heated inclined surfaces are essentially absent" [57]. The remaining portion of this chapter is a chronological brief summary of the articles pertinent to natural convection from upward facing heated machined flat plates.

B. R. Rich published an analytical analysis in 1953 which predicted free convection heat transfer rates from an upward facing inclined heated plate [41]. The results of this analysis showed that the Nusselt number for an inclined plate could be predicted by using a vertical plate correlation except that the Grashof number should be calculated on the basis of the component of acceleration of gravity along the plate surface. Through experiments conducted using a Mach Zehnder interferometer, the analytical results for laminar flow were confirmed. This analysis has been widely accepted and can be found in most heat transfer texts [27, 32].

D. J. Tritton investigated natural convection from horizontal and inclined plates in 1962 [48, 49]. The major emphasis in these

articles was the flow phenomena of turbulent free convection and their variation with the angle of inclination. The conclusions of these articles were that slight inclinations from the horizontal did not alter the heat transfer from the plate or the mean temperature distribution in the heated air. Furthermore, it was determined that there was a marked dependency between the onset of transition from laminar to turbulent flow and the angle of inclination.

In 1968, W. T. Kierkus published a perturbation analysis on two-dimensional laminar free convection from an inclined plate to fluid with a Prandtl number of 0.70. This method used the classical boundary layer solution as the zeroth order approximation [31]. One inclined plate experiment was conducted and good agreement was obtained with the analysis.

Also in 1968, Sparrow and Husar performed flow visualization experiments using a pH technique on an isothermal plane [46]. From these experiments it was determined that for angles greater than 15 degrees from the vertical a cellular secondary flow is superposed on the natural convective flow. This secondary flow consists of longitudinal vortices which constitutes the first state of the laminar to turbulent transition. This behavior is in contrast to Tollmien-Schliching wave which constitutes the first stage of transition on a vertical plate. It was also determined that the number of these vortices increases with an increased temperature difference but the number of vortices is relatively independent of angle.

A major contribution in measurement of heat transfer

coefficients in laminar, transitional and turbulent natural convection from inclined plates was C. G. Vliet in 1969 [51]. The experimental investigation was conducted using a constant heat flux plate. Most tests were conducted using water as the convective media although two tests were performed in air. In the laminar regime Vliet's results coincided with those of Rich [41]. In transitional flow it was concluded that the location of transition was strongly dependent on angle of inclination and that the span of the transitional regime was approximately 1.5 orders of magnitude of the Grashof number. In the turbulent regime it was determined that there was better correlation between the Nusselt and Grashof number if the actual acceleration due to gravity was used rather than the parallel component to flow as in laminar regimes.

Also in 1969, J. R. Lloyd and E. M. Sparrow published the results of the experiments relating the nature of natural convection flow instability to the angle of plate inclination [36]. Using an isothermal inclined plane it was concluded that the mode of instability was due to waves for angles of inclination less than 14 degrees from the vertical and that longitudinal vortices were the mode of instability for angles greater than 17 degrees. Also the angular dependency of the Rayleigh number characterizing the onset of instability for inclinations up to 60 degrees was determined.

In 1970 K. E. Hassan and S. A. Mohamed published the results of an experimental investigation of free convection from an isothermal inclined plate. The local Nusselt number was shown to be a function

of the local Grashof number modified by the cosine of the angle of inclination for laminar flow. However, toward the trailing edge of the inclined plate a region of separated flow occurred which continued to give the Nusselt number an angular dependency. In all regions up stream of the separated region the results were in close agreement with established theories of laminar flow heat transfer.

J. R. Lloyd, E. M. Sparrow, and E. R. G. Eckert in 1971 published a paper [35] concerned with results of experiments conducted in natural convection mass transfer adjacent to vertical and upward facing inclined planes. Mass transfer rates in transitional and turbulent regimes were presented. In the transition regimes significant spanwise variation in both instantaneous and time averaged measurements for angles of inclination greater than 15 degrees were measured. In the turbulent regime the local nondimensional mass transfer rates correlated well with the Rayleigh number to the one-third power.

In 1972, T. Fujii and H. Imura published the results of experimental measurements of heat transfer coefficients from inclined planes [16]. This article confirmed Vliet's [51] conclusion that there was no angular dependency of Nusselt number in the turbulent regime and, like Lloyd, et al.[35], that the heat transfer coefficient was shown to be independent of length.

CHAPTER III

TEST APPARATUS

The test apparatus consists of five basic elements: heated plate, plate carriage, thermocouples and potentiometer - recorder, heaters and power supply, and camera - interferometer.

The heated plate was a 60 x 10 x 1/2 inch aluminum plate with a leading edge milled to an angle of 30 degrees with respect to the upward facing plate surface. The upward facing surface of the plate was polished to a smooth finish and all burrs were removed from the sides of the plate.

The plate was heated by 10 segmented 6 x 10 inch Watlow silicone rubber heaters which were attached to the back of the plate by GE RVT. 116 adhesive. The reason segmented heaters were employed is because the heat transfer coefficient shows a large variation in magnitude from the leading edge to downstream locations. Figure 2 graphically depicts this variation in heat transfer coefficient from a heated vertical plate. In order to obtain an isothermal plate it is necessary to increase the heat flux close to the leading edge of the plate and reduce it in the direction of flow.

The large exposed back surface of the heaters was insulated with one-half inch fiberglass batten insulation to reduce the heat loss from the back surface of the plate.

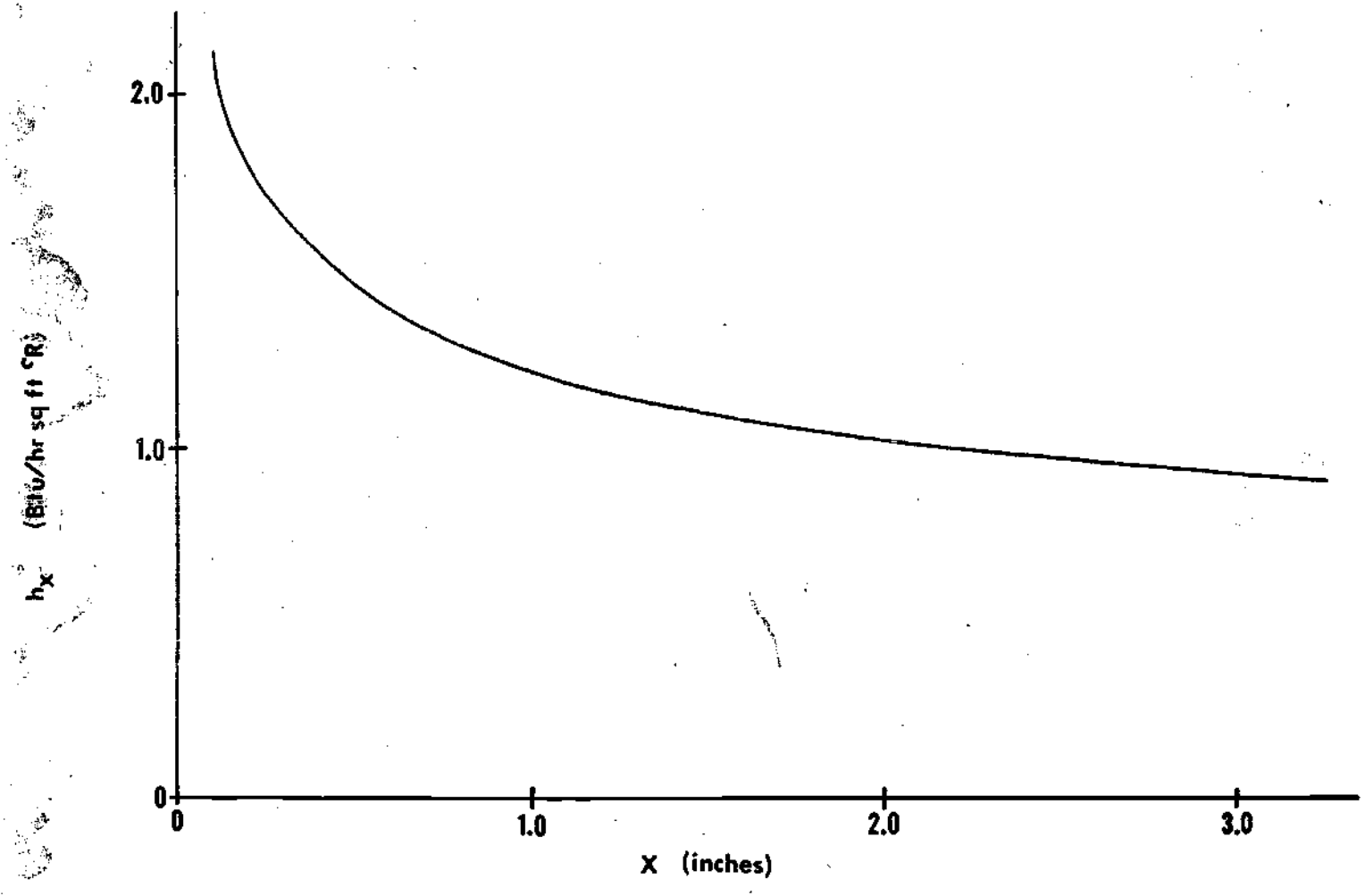

Figure 2. Local Free Convective Heat Transfer Coefficients from a Vertical Isothermal Plate. Ref. [8].

Because the viewing section of the interferometer was only 3 3/4 inches in diameter and the plate was 60 inches long, it was necessary to mount the plate on a carriage-rail system. This system permitted the plate to be moved through the test section and also rotated from an inclination of 45 degrees from the vertical to a horizontal position. See Figure 3. The rail system also had vertical side surfaces attached to prevent significant side flow from occurring across the plate surface. A reference marker was fixed to the side of one rail in the viewing section so that it was visible in all pictures taken. Also a scale was marked on the carriage so that plate position within the test section could be accurately determined.

The temperature sensing system consisted of 21 copper-constantan thermocouples mounted from the back of the plate to a position 3/64 inch from the upward facing surface. Each thermocouple bead was covered by a film of RTV 116 to insulate the thermocouples from the A. C. noise of the heaters. Seventeen thermocouples were mounted along the longitudinal axis and four were mounted 2.5 inches off this axis. A diagram of the thermocouple locations appears in Appendix B.

Sixteen thermocouples, 14 on the center axis of the plate and two off center, were continuously monitored with a Honeywell Electronik 153 multipoint recorder. A Leads and Northrup Potentiometer was wired into this circuit in order to check the accuracy of the recorder and to provide proper scaling of the recorder. (Schematic, Appendix B).

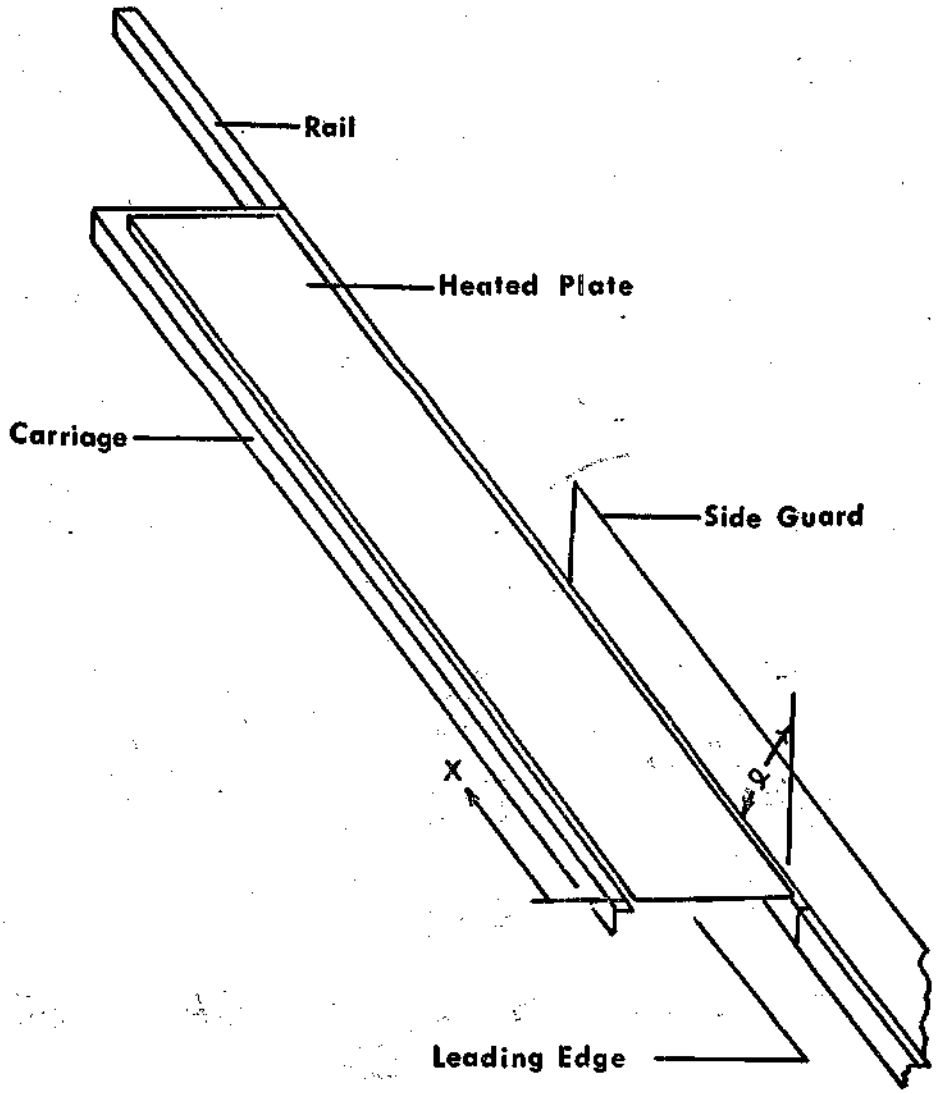

Figure 3. Schematic Diagram of Plate System.

The air temperature was monitored by two thermocouples placed five feet from the ends of the plate and shielded for radiation from the plate. These were not continuously monitored by the recorder but were measured before and after each test.

The power supplied to the heaters was regulated by seven A. C. variacs. The first five heaters from the leading edge were each wired to a single variac. The next two heaters were wired in parallel to the sixth variac and the last three heaters were similarly wired to the seventh variac. By monitoring the temperature on the recorder, the power input to the heater was adjusted to insure isothermal plate conditions.

The fifth system is the differential interferometer-camera systems. The differential interferometer is an optical instrument that permits the measurement of the gradient of index of refraction in the viewing section. Only a brief overview of its application in measuring heat transfer coefficients will be discussed. For a more detailed discussion the reader is referred to references [5, 6, 8].

A schematic diagram of this interferometer is shown in Figure 4. Basically light leaves the light source and is filtered to obtain a single wave length. It then passes through a polarizer oriented so that the light is divided into two equal magnitude electrical vectors. These two vectors are focused on the first of three Wollaston prisms, WP1. The Wollaston prism causes the rays associated with each electric vector to diverge slightly as they leave the prism. WP1 is at the focal point of the first spherical minor, SP1, so that after

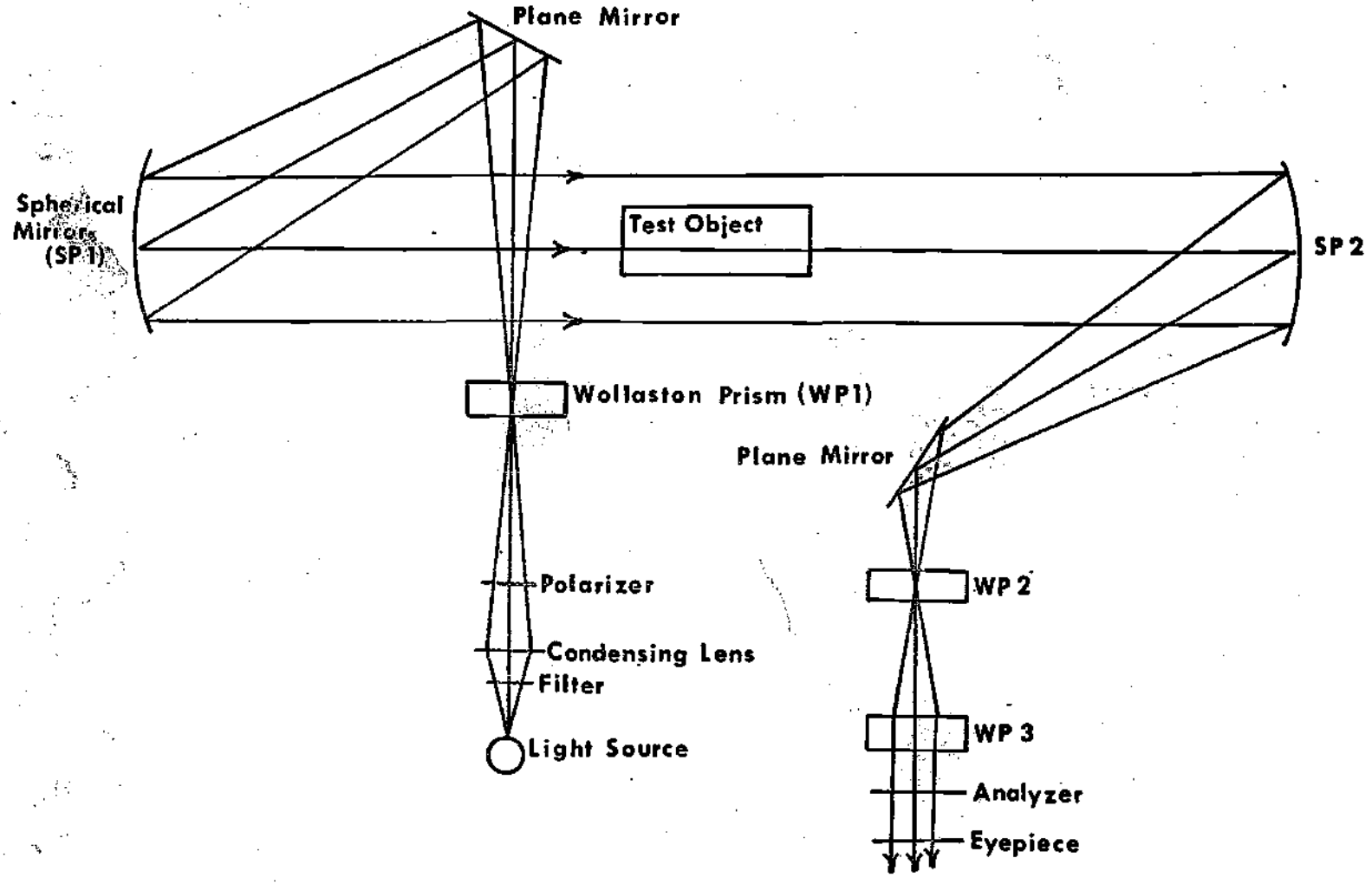

Figure 4. Schematic Diagram of Differential Interferometer.

reflection from the mirror the two rays have parallel but slightly different paths. After the rays pass through the test section they are focused on the second Wollaston prism; WP2, which is the same as the the first prism but rotated so that the effect of the first is reversed. Leaving WP2 the rays pass through the third Wollaston prism, WP3. This prism produces a phase shift between the two vector components. After leaving the third Wollaston prism, WP3, the rays pass through an analyzer which causes interference between the two electric vectors. The interference pattern produced is a series of equally spaced parallel fringes which is commonly referred to as a parallel fringe interferogram. All prisms can be rotated so that measurements can be made in any direction.

When a heated object is located in the test section, the two slightly separated rays pass through regions of slightly different temperatures. As a result the two rays experience slightly different optical paths which cause a deflection in the fringe pattern produced by the third Wollaston prism. This deflection of an individual parallel fringe is proportional to the gradient of the index of refraction experienced within the air surrounding the heated plate. This gradient can be related to the temperature gradient which in turn, by using Newton's "Law of Convection," can be related to the heat transfer coefficient "h". The governing equation for this relation is:

$$h = \left[\frac{k_s R T_s^{\,2} \lambda}{3GPLg\Delta n\theta (T_s - T_a)} \right] m$$

Again the advantage of using a differential interferometer is this direct correlation between the heat transfers coefficient "h" and the fringe shift "m". Details of the derivation of this equation may be found in reference [5, 6, 8].

Figure 5 shows a sketch of a typical parallel fringe pattern produced by free convection from a flat inclined plate. The fringe deflection at the plate surface is proportional to the local free convective heat transfer coefficient.

The third Wollaston prism may be removed so that the only fringes that appear are those caused by a gradient of index of refraction in the test section. This condition produces fringe lines which are proportional to lines of constant gradient as shown in Figure 6.

The camera used to record the fringe pattern was a Bolex H-16 Reflex camera which was rigidly mounted to the eye piece of the interferometer. A film speed of 18 frames a second was used with a shutter setting of 1/2 closed position. Kodak 4-X film 7277 with an ASA of 320 was used for all tests. Since the camera collected all of the light from the mercury arc source two Kodak N. D. 0.80 and one 0.60 gelatin nutral density filters were used to obtain proper film exposure.

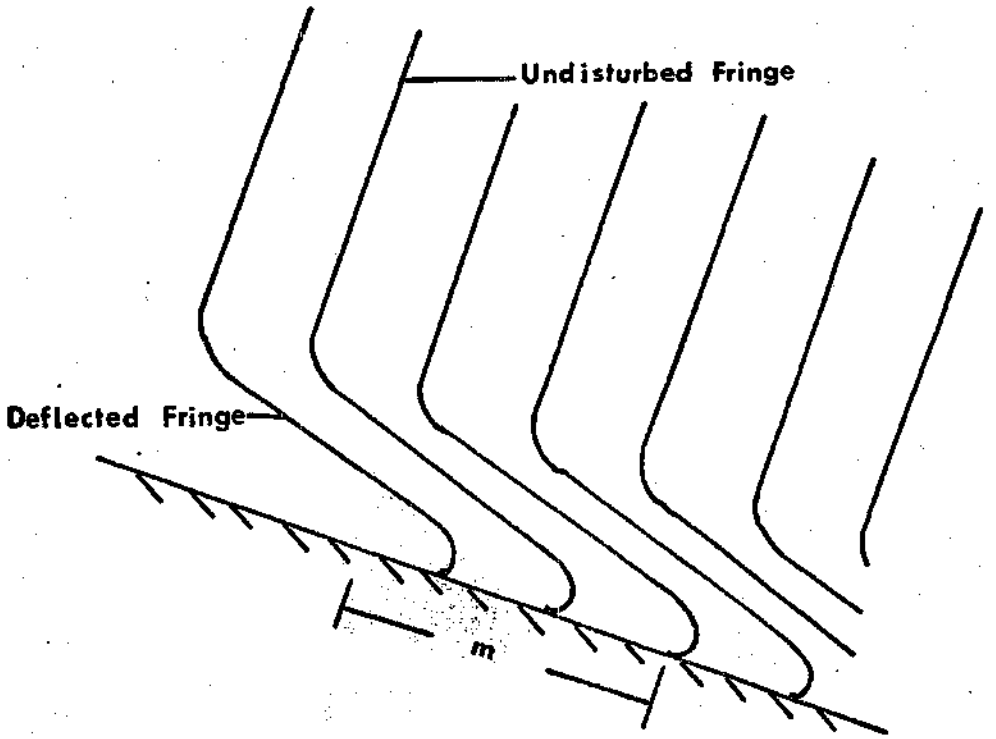

Figure 5. Schematic Diagram of Parallel Fringe Pattern.

CHAPTER IV

TEST PROCEDURE

Prior to conducting the experiment all ventilation ducts in the room were sealed with metal plates and flaps were placed around all door edges to insure against outside circulation effects. Before each test was conducted the following procedure was followed:

(1) The Honeywell recorder and potentiometer were calibrated.

(2) The plate angle was set by use of plumb bob and protractor to less than one-half degree of desired angle.

(3) The plate and interferometer alignment were checked.

(4) A reference picture of the parallel fringe pattern was taken.

(5) The plate was moved to initial test position and the angle of inclination and alignment were rechecked.

After these preliminary steps were taken the plate was heated and power settings were adjusted to obtain isothermal conditions. Once the plate had stabilized to the desired temperature a comparison of thermocouple EMF measured by the recorder and potentiometer was conducted. Room air temperature and pressure were measured at this time. Motion pictures were taken at the desired position along the plate surface. Normally these positions were spaced from four to six inches apart and pictures were taken of both the infinite and parallel

fringe settings at each location. During this period of plate movement the temperature was continually monitored to insure that the plate temperature did not vary by more than three degrees Fahrenheit.After the test run was completed, but prior to turning off the plate, another comparison was made of the EMF's measured by the recorder and the potentiometer.

The plate temperature was determined by averaging the temperature readings of all the thermocouples at five different times during the period of the test run and corrected by the average variation between the recorder and potentiometer. (See Appendix D for plate temperature data). The average air temperature was determined by averaging the five air temperature readings.

To determine the fringe shift, the reference parallel fringe pattern was projected on to a screen and deflection measurements were taken by superposing test frames on the reference pattern. Computation of the average fringe shift was achieved by time averaging the fringe shift of every third frame for a total of one-half second in the laminar region and for a total of five seconds in the transitional and turbulent regimes. It was found that there was little difference in the average fringe shift if a period of five to ten seconds was used.

All air property values were based on a reference temperature which was the average between ambient air and plate temperature, $T_f = (T_a + T_s)/2$. Property values tabulated from reference [32, 56] are discussed in Appendix E.

CHAPTER V

DISCUSSION OF RESULTS

All tests were conducted in air, Pr = 0.696, on an isothermally heated upward facing inclined plate at a temperature of approximately 280°F. All heat transfer results were measured between two and 49 inches from the leading edge of the plate. Four tests were conducted, one each at 45°, 60°, 70°, and 80° from the vertical. Since the primary objective of this investigation was the measurement of heat transfer rates in the transitional and turbulent flow regimes, the plate temperature was selected to insure that as large a portion of the plate as possible would be in these regimes. This procedure led to the selection of 280°F as the plate temperature for all test runs. See Appendix C for details.

The discussion of experimental results will be presented in two sections: Flow Visualization and Heat Transfer.

Flow Visualization

One very important benefit of using an interferometer is the fact that the fringe patterns permit visual observations of the flow of heated air surrounding the plate. The infinite fringe interferogram provides an instantaneous photograph of the thermal boundary layer. As a result it is a relatively simple task to determine at what distance from the leading edge of the plate flow proceeds into

the transitional and fully turbulent regime. Also fluctuations of the flow pattern in the transitional and turbulent regime which can cause large variations in the local heat flux from the surface can be observed with the aid of the infinite fringe photograph. The parallel fringe pattern can then be utilized to determine the magnitude of the variation in the convective heat transfer coefficient.

A study of the infinite fringe patterns of the heated air surrounding the inclined isothermal plate was initiated to determine several parameters which are important in the study of heat transfer from the plate. The thermal boundary layer thickness for the 45° inclined plate was determined for a position from the leading edge of the plate until the thickness became greater than the field of view of the interferometer. Values of critical Rayleigh numbers as a function of plane inclination were calculated which estimate the onset of transitional and fully turbulent flow. Also measurements taken from the infinite fringe photographs were used to determine the frequency at which waves were shed from within that position of the boundary layer adjacent to the plate.

The onset of transitional flow was first marked on the infinite fringe photographs by an apparent whiff of heated air which repeatedly rose from the surface and disappeared in the outer regions of the boundary layer. Lloyd and Sparrow [36] and Sparrow and Husar [46] indicate that transition on planes inclined greater than 17° from the vertical is caused by the formation of longitudinal vortices. The whiffs of heated air observed in the interferograms which were oriented

parallel to the plate could be the indication of the heated air rolling out of such vortices. The location where this phenomenon occurred and the measurement of the Rayleigh number corresponding to this location correlated well with Lloyd and Sparrow's [36] critical Ra_x for onset of transition, see Table 1. Also in this table are the observed critical Ra_x for angles of 70° and 80° which were not covered by Lloyd and Sparrow.

Both infinite and parallel fringe patterns could be used to indicate the onset to transitional flow. The infinite fringe pattern graphically portrays the flow structure and provides a visualization of particle movement which is easy to interpret. However, it was much easier to isolate the onset of transitional flow by using the parallel fringe pattern because of the contrast produced in fringe lines. The disturbance in the fringe lines produced oscillations which were easy to observe.

Once transition occurred the flow rapidly took on the appearance, in the infinite fringe photograph, of an outer core region of rapidly varying mixing and a thin sub-layer close to the wall of more steady wave-like motion. (A photograph depicting this is shown in Figure 6a and 6b). In the transitional and turbulent regimes, waves occurred in the sub-layer region. These waves moved up the plate and into the outer core where the motion of heated air was more turbulent. The tops of these waves appeared to roll off of the slowly fluctuating sub-layer and on into the more random motion of the core fluid.

The frequency of these "wave bursts" was not dependent on their

Table 1. Comparison of Critical Ra_x for Transitional Flow.

Angle	Lloyd's Mean Ra_x	Lloyd's Stand Deviation	Observed Ra_x
45°	1.7×10^7	$\pm 0.79 \times 10^7$	2.4×10^7
60°	7.7×10^5	$\pm 4.6 \times 10^5$	2×10^6
70°	-		3×10^5
80°	-		2×10^4

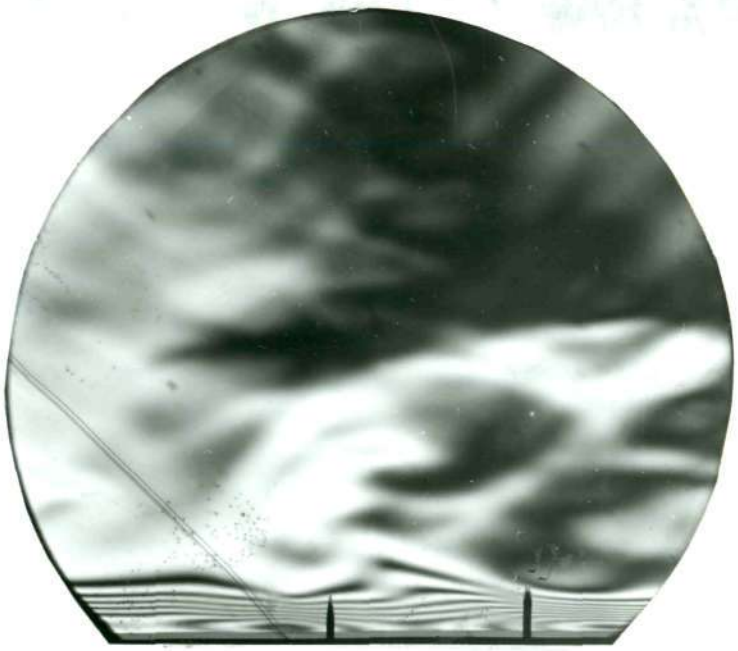

Figure 6a. Infinite Fringe Photo of 45° Inclined Plate at $Ra_x = 7.2 \times 10^9$.

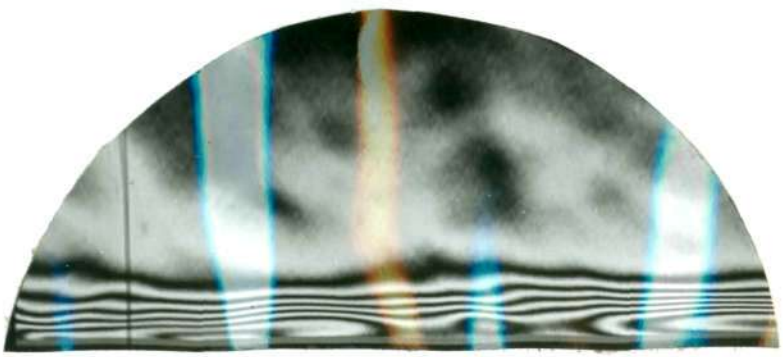

Figure 6b. Infinite Fringe Photo of Horizontal Plate at $Ra_x = 7 \times 10^8$.

location on the plate, but the frequency randomly varied as much as ± 30 percent. The angle of plate inclination did not appear to greatly effect the frequency, though the frequency of occurrence was highest for the 70° plate at approximately 1.8 waves per second and lowest for the 80° plate at about 1.2 waves per second.

Determination of the threshold of fully turbulent flow was much more difficult than locating the position where transition first occurred because the outer portion of the thermal boundary layer already appears as though a significant amount of mixing was occurring only inches from position of transition onset. Flow visualization criteria for determining turbulence should be universal or at least indications of turbulence should be the same regardless of test. But in using the infinite fringe there was very little in the area of suspected turbulence that would distinguish the turbulent flow structure from the transitional flow just slightly up stream.

Due to this difficulty in observing the occurrence of fully turbulent flow with the infinite fringe pattern, the parallel fringe pattern was eventually used and provided a much better measure of the onset of the turbulent flow regime. In each case the outer portion of this fringe pattern which was not greatly deflected in the transitional regime was forcefully disturbed in the turbulent area. The presence of a wave bust associated with the constant gradient sub-layer caused the relatively undisturbed fringe in the outer layer to oscillate much more violently than had occurred in the transitional regime. The initial onset of these forceful disturbances coincided quite well with

relatively large variations in the local instantaneous convective heat transfer coefficient. These variations were characteristic of the flow fluctuation which occurred in the turbulent area, see Figure 10.

The span of transitional regime was found to be of the order of two to three magnitudes of Ra_x as compared to Vliet [51] who determined the span to be of the approximate order of 1.5. There appears to be no conflict in these conclusions. One possible reason can be offered for this difference. Vliet used a probe of copper constantan thermocouples for detecting flow oscillations as opposed to an optical device which is more sensitive to any rapidly changing disturbance.

The thickness of the thermal boundary layer could be easily measured from the infinite fringe photograph because the region within which there were any thermal gradients were outlined by the presence of fringe lines. However, this measurement was limited to regimes near the leading edge of the plate because the boundary layer grew quite rapidly and was soon out of the field of view. The boundary layer thickness for the 45° plate is plotted in Figure 7 until a location at which the outer edge of the boundary layer was no longer visible.

A study of the infinite fringe pattern, Figure 8, revealed an unexpected result. Even though the outer extent of the thermal boundary layer grew quite rapidly as indicated in Figure 7, there was a sub-layer close to the plate surface within which the temperature of the fluid changed quite rapidly. Interestingly enough, this sub-layer

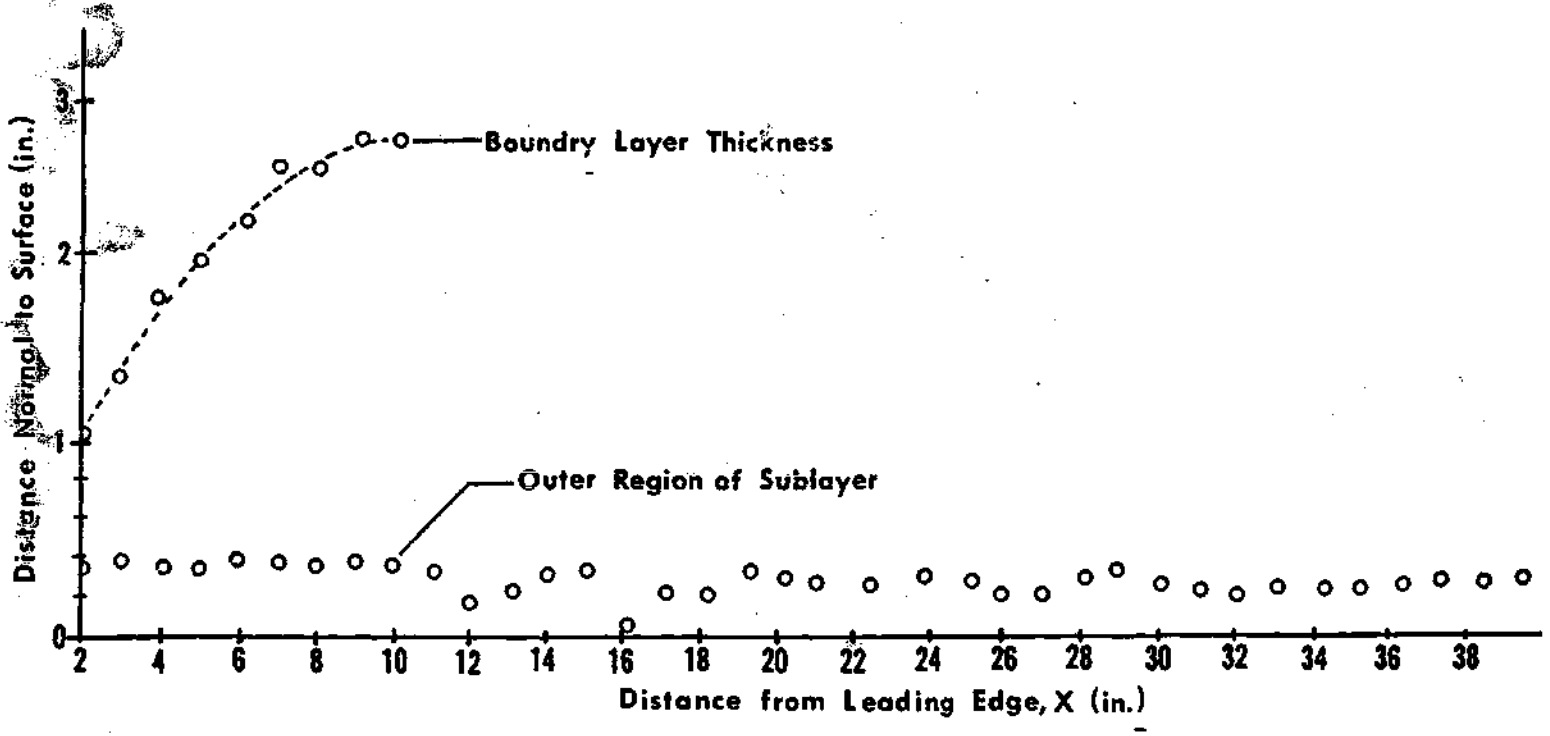

Figure 7. Boundary Layer and Outer Region of Maximum Gradient Sub-layer for 45° Inclined Plate.

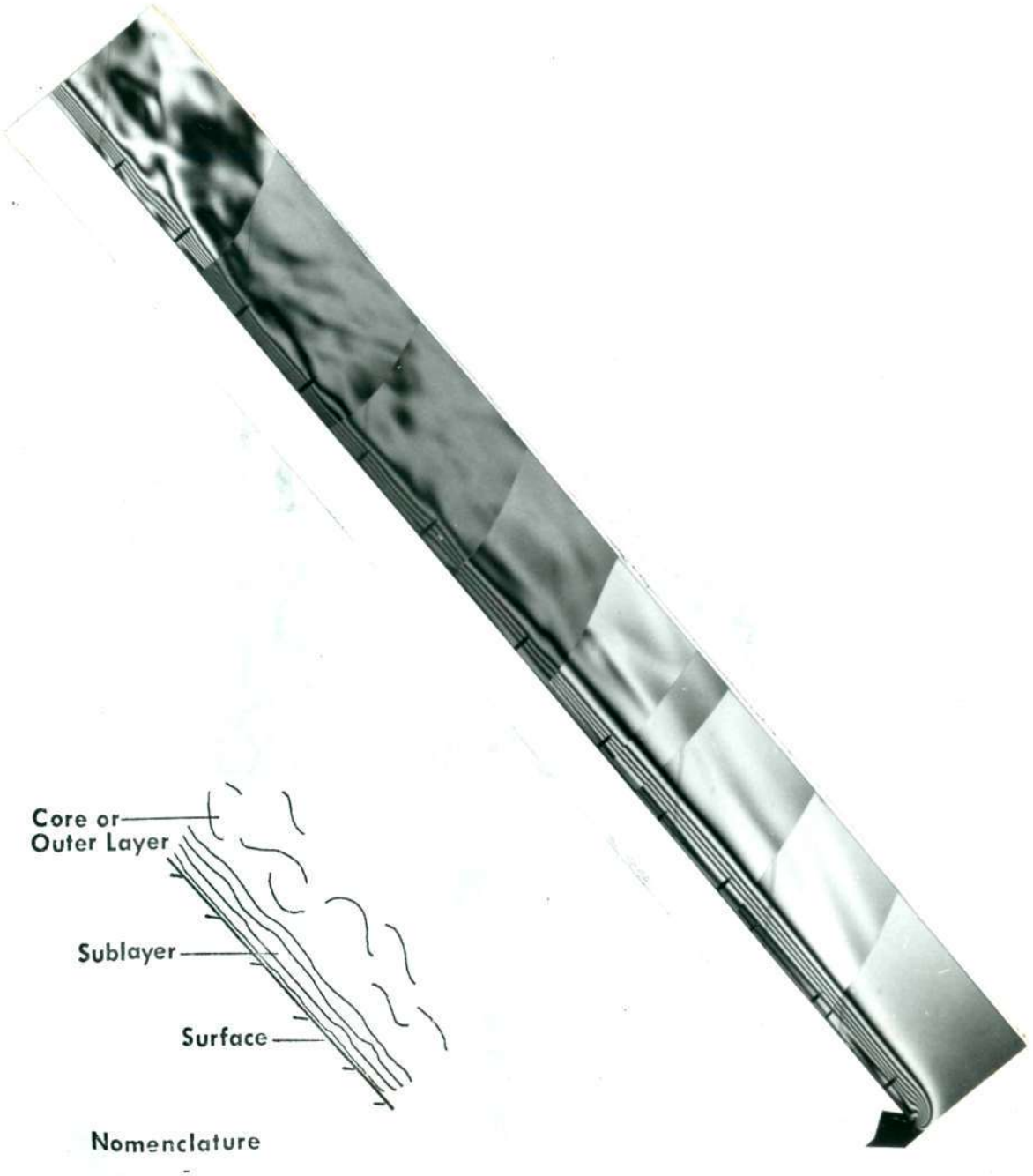

Figure 8. Composite Infinite Fringe Photo of 45° Inclined Plate.

remained fairly uniform in thickness for all locations over the surface of the plate. The extent of the sub-layer can be seen as several closely spaced fringe lines that are parallel to the plate. In the laminar regime the sub-layer remained very stable and uniform in thickness except at the leading edge of the plate. In the transitional regime, the occurrence of waves first appeared in the outermost region of this sub-layer although the average thickness of the sub-layer still remained much the same as in the laminar portion of flow. Even into the fully turbulent regime the thickness of sub-layer remained constant with intermittent disturbances caused each time a wave moved along the surface of the plate. This disturbance and its effect on the surrounding flow pattern and on the heat transfer at the surface was more intense in the fully turbulent regime than in the transitional regime. A plot of the instantaneous thickness of the sub-layer is shown in Figure 7.

Hassan and Mohamed [26] and Dr. Hassan in personal conversations indicated that there is good reason to believe that the flow characteristics on an inclined plate and a horizontal plate would be similar in the turbulent regime. Infinite fringe photographs of a horizontally heated plate and a 45° inclined plate were studied to confirm this prediction. In Figure 6 two infinite fringe pictures are shown with one illustrating the fringe pattern for a horizontal plate and one for a plate inclined at 45°. Both photographs have striking similarities. Both show small cells next to the surface, a wavy band of constant gradient lines spaced just above the surface,

and an outer region of more thoroughly mixed fluid. One dissimilarity can be detected however. In the 45° photograph the effect of the bouyancy force moving the wave up the plate appears while in the horizontal orientation the flow moves primarily away from the surface.

Heat Transfer Measurements

The parallel fringe pattern produced by the differential interferometer was used to measure the local convective heat transfer coefficient in the laminar regime and the local instantaneous heat transfer coefficient in the transitional and turbulent regimes. The local instantaneous values in those regions in which the heat transfer coefficient varied with time were integrated to obtain time average local heat transfer coefficients. Data collected in this manner was then compared with existing results for the laminar regime and a correlation of the form of $Nu_x = C(Ra_x)^n$ is proposed for the turbulent regime.

The length of plate under the influence of laminar flow has been shown to be a function of the angle of inclination of the plate. As confirmed in Table 1, the position from the leading edge to the point of onset of transitional flow decreases as the angle of plate inclination increases.

Due to the rather small percentage of plate surface subjected to laminar flow, particularly for the highly inclined plates, the number of data points recorded for laminar flow is rather small. Several of these data points are shown in Figure 9 for laminar flow for a 45° inclined plate.

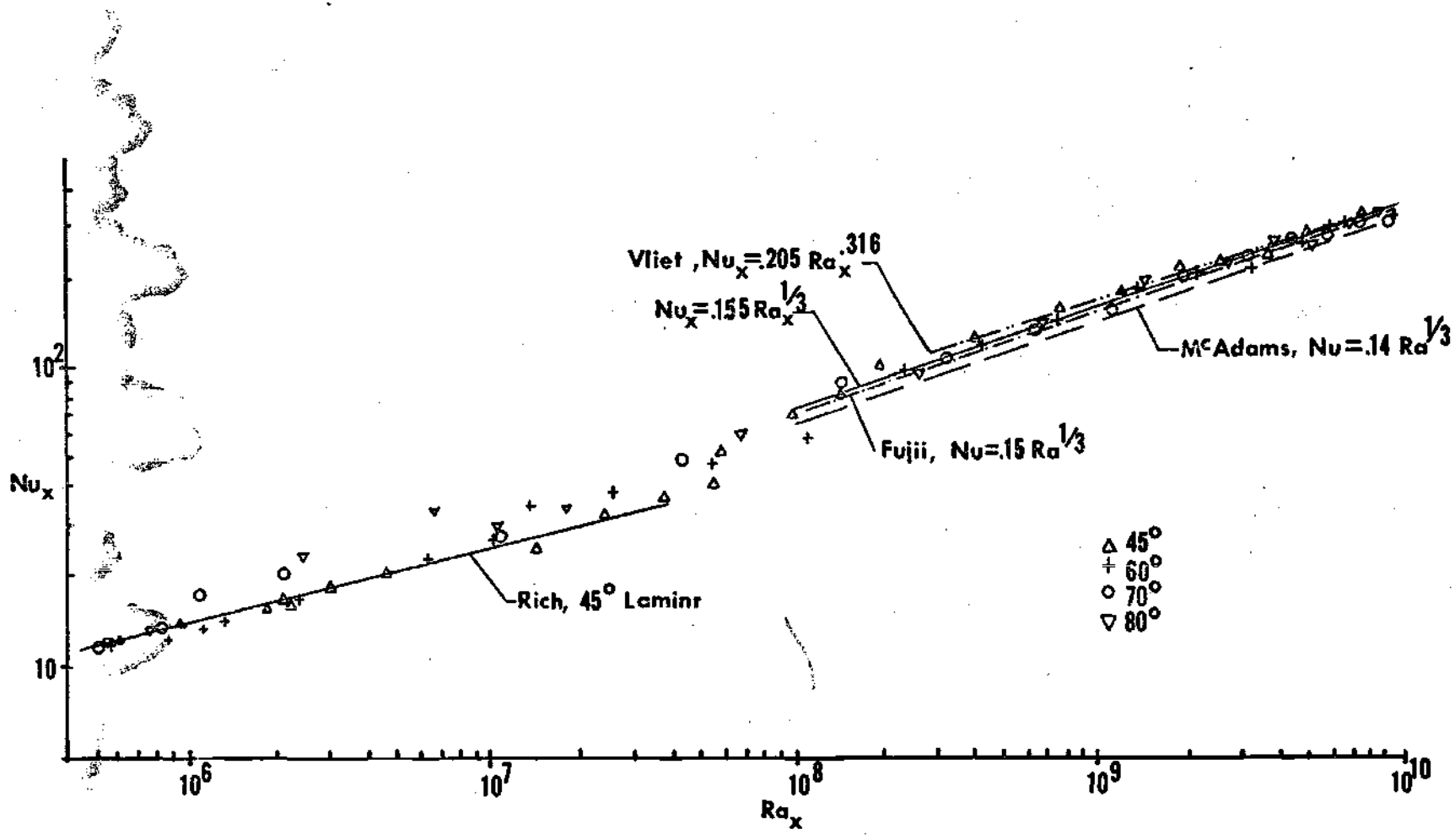

Figure 9. Graph of Nu_x as a Function of Ra_x for Inclinations Investigated.

A comparison of the local Nu_x obtained in this experiment with Rich's correlation [41] shows a deviation of less than 10 percent except for one point in the laminar regime. See Appendix F for comparison.

The local Nu_x in the transitional regimes fluctuated considerably and there is insufficient data to show any firm conclusions, but the plot of this data in Figure 9 is quite similar to the graphical plots of Vliet and Lui [52] for Nu_x in the transitional regime on a vertical plate. Furthermore, the data in the transitional regime did tend to correlate better when using $Ra_x \cos \alpha$, where α is the angle of inclination measured from the vertical, than when using Ra_x alone. This is what Hassan and Mohamed [26] contend. However, the present study did not yield sufficient data to do more than state that the correlation in the transitional regime does show some angular dependency.

The presence of a wave occurring inside the thermal boundary layer which was first mentioned in the flow visualization section could be observed in the parallel fringe pattern. The general trend during the observed presence of one of these waves was an increase in the deflection of the parallel fringes immediately below and up stream of the wave location by as much as 50 percent more than those deflections down stream of the wave, Figure 10. Thus, the presence of the wave caused increases in the local instantaneous heat transfer coefficient of as much as 50 percent over the immediate down-stream coefficient.

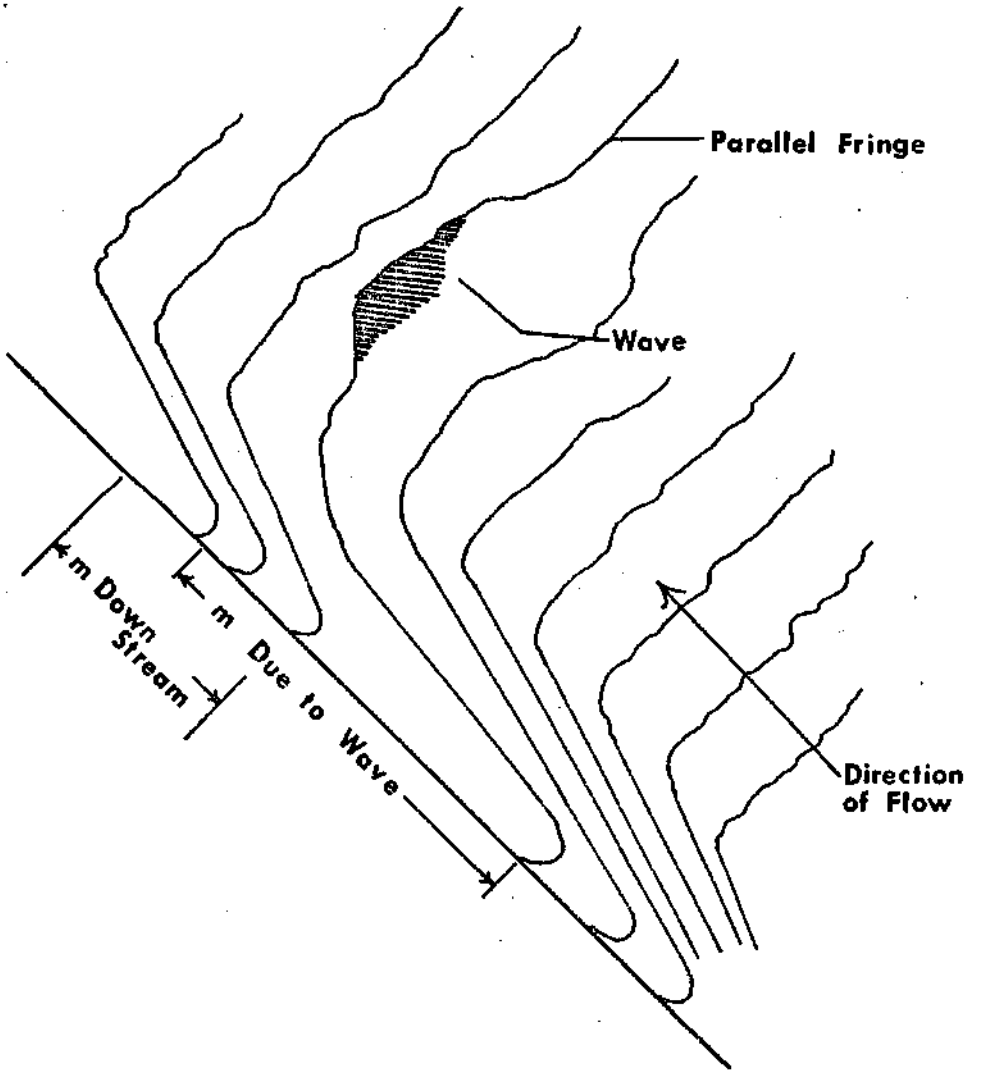

Figure 10. Relative Effect on Fringe Deflection Due to the Presence of a Wave.

In Figure 11 the instantaneous local heat transfer coefficients for a given Ra_x in the turbulent regimes are plotted for the four angles of plate inclination investigated. The plot of these coefficients is completely random with no apparent periodic cycle. However, one can see the effect that the presence of a wave has on the heat transfer coefficient. The times at which the heat transfer coefficient reached a maximum coincided with the presence of stronger waves. Referring to the 45° plot one can see that strong waves occurred at this location of interest at 1/2, 2 1/2, 3 1/3 and 4 1/6 seconds during the five-second time interval that the flow was observed creating a variation of as much as $\pm$ 40 percent in some cases and a variation of + 26 percent and - 30 percent from the time averaged heat transfer coefficient for the five-second interval shown in Figure 11.

Experimental results from all time averaged local instantaneous heat transfer coefficients in the turbulent regime indicate that there is no length or angular dependency in the heat transfer coefficient for a plate inclined between 45° and 80° from the vertical and

$$Nu_x = .155\ Ra_x^{1/3}$$

provides a best fit for this data. (Appendix H gives criteria for best fit curve). This result is within 3.5 percent agreement with Fujii [16], see Figure 9 and in agreement with Lloyd, et al. [35] who observed neither angular or length dependency for the heat transfer coefficient in the turbulent regimes. While Vliet [51] also indicates

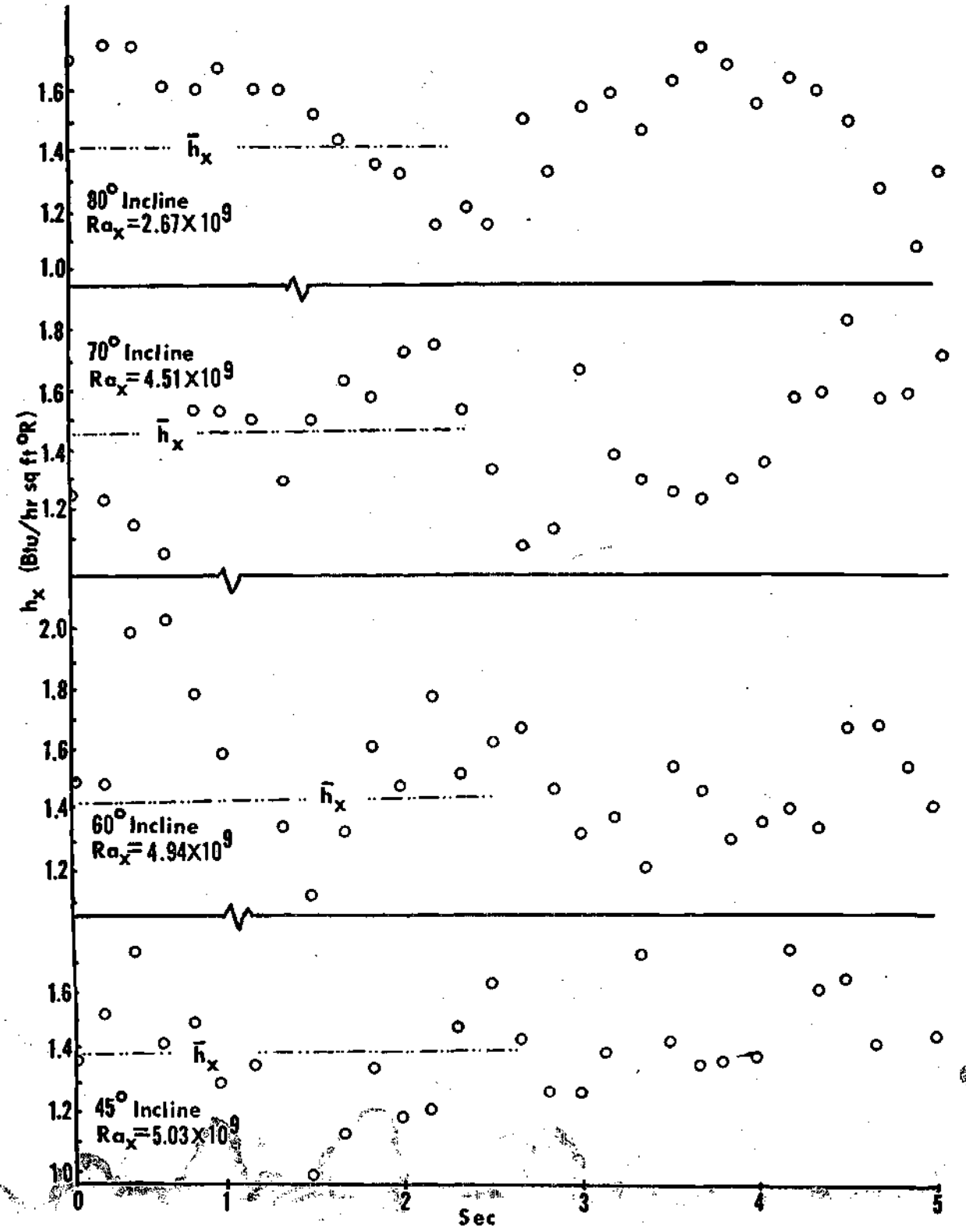

Figure 11. Plot of Instantaneous Heat Transfer Coefficients.

that there is no angular dependency in the turbulent regime, he did find a slight length dependency of

$$Nu_x \propto Ra_x^{.316}.$$

However, in the range of Ra investigated there is good agreement between experimental data collected during this study and Vliet's curve, Figure 9.

Furthermore, recalling Hassan's conversation concerning the similarity between flow in the turbulent regime from inclined and horizontal plates, a comparison was made between the present data and McAdams' [39] Nu equation

$$Nu = .14\ (Ra)^{1/3}$$

for free convection from an isothermal horizontal flat plate. The present results predict a Nusselt number that is 10.7 percent higher for a given Ra_x than that which would have been obtained from McAdams' equation which is also plotted in Figure 9. This variation is well within the 20 percent accuracy that Krieth [32] claims can in practice be predicted by experimental data.

Lloyd, et al. [35] employed a technique of plotting the $Sh/Ra_x^{1/3}$ as a function Ra_x to indicate a range of Ra_x over which the flow can be assumed to be fully turbulent for mass transfer from a flat inclined plate. By following a similar procedure, one can determine the range of

Ra_x for which the flow from a heated inclined plate becomes fully turbulent. If the dimensionless parameter $Nu_x/Ra_x^{1/3}$ is plotted as a function of Ra_x, regions where the data points lie along a horizontal line indicate that the heat transfer coefficient is independent of distance from the leading edge of the plate. Since the behavior is indicative of turbulent flow, this criteria can be used to approximate regions of turbulent flow. In the studies of Vliet, Lloyd and Hassan mentioned previously, this approach has been used to determine the onset of fully turbulent flow. This technique was used for the present study and the results appear in Figure 12. From this figure two observations can be made: Nu_x for all angles of inclination approach a similar dependency on Ra_x, and that the critical Ra_x which locates onset of fully turbulent flow decreases as the angle of plate inclination increases. Figure 11 was used to identify the onset of the turbulent regime. The critical Ra_x measured by this method is indicated in Figure 12 and tabulated in Table 2 where the Ra_x denoting onset of transitional regime is repeated for completeness.

Four data points in the transitional-turbulent regime were reevaluated to insure the technique of reading fringe shifts was accurate and to assure reproducibility of data. The same portion of the film strips were used, but data was not collected from the same portion of the film. The difference in fringe readings for these four points were less than 2 percent. Comparison is given in Appendix I.

An attempt was made to check the plate temperature by integrating the area under a deflected fringe with the aid of a planimeter.

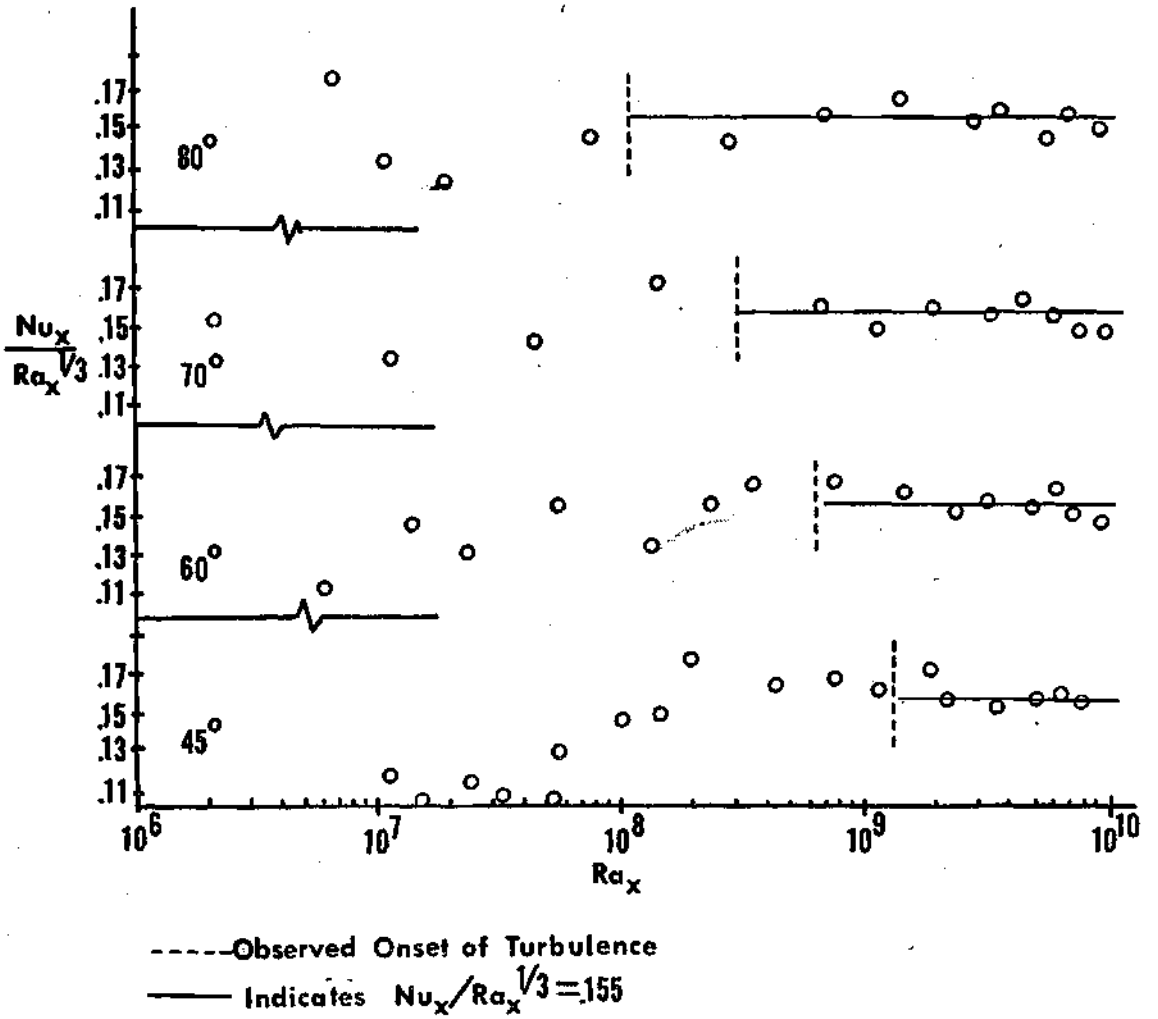

Figure 12. Plot of $Nu_x/Ra^{1/3}$ as a Function of Ra_x.

Table 2. Critical Ra_x for Onset of Transition and Turbulent Flow.

Angle	Ra_x Transition	Ra_x Turbulent
45°	2.4×10^7	1.45×10^9
60°	2×10^6	6.2×10^8
70°	3×10^5	2.8×10^8
80°	2×10^4	1.0×10^8

Difficulty arose in the measurement of small areas under the fringe with the result that the calculated wall temperatures varied by ± 50 percent when compared to actual temperature measured by means of thermocouples embedded in the plate surface. This result suggests that the differential interferometer has serious limitations if one wanted to convert the intended function of the fringe lines from a measurement of temperature gradient to one of measurement of temperature by integrating areas under the deflected fringe lines. However, it is possible that the figure of a 50 percent error in temperature measurement could be reduced by more careful integration techniques and a better method of projecting the fringe pattern so that the area to be integrated is of reasonable size.

CHAPTER VI

CONCLUSIONS

The differential interferometer can be employed to determine the instantaneous local and average local heat transfer coefficients in the laminar, transitional, and turbulent regimes of natural convective flow.

In the turbulent regime the heat transfer coefficient showed no apparent dependency upon angle of inclination or length from leading edge for angles of inclination between 45° and 80°. The results from experimental data provide a relatipnship of

$$Nu_x = 0.155\ Ra_x^{1/3}$$

for the fully turbulent regime at angles of inclination of 45° to 80°.

The instantaneous heat transfer coefficient in the turbulent regime fluctuated randomly and did not show a predictable cyclic nature. Typical local instantaneous heat transfer coefficients in the turbulent regime varied by as much as $\pm$ 40 percent. This variation was due to "wave busts" observed in the flow.

CHAPTER VII

RECOMMENDATIONS

The method of heating the plate by using segmented electrical heaters to achieve isothermal conditions worked very well and was simple to construct and operate. However, warm up time took approximately four hours to insure that the plate was at the proper and stable temperature.

The rail system was not designed properly and consideration should be given to employing wheels or bearings between carriage and rails. Also any future design should attempt to eliminate flexing that was present in the rail system.

Further investigation should be conducted using the differential interferometer to determine what visual criteria can be used to guarantee the existence of fully turbulent flow. Infinite and parallel fringe patterns produced during this investigation give an indication that fully turbulent flow is based on the intensity of the mixing which was visible by the oscillations of the parallel fringes. Further investigation is needed in this matter.

Secondly, an investigation should be conducted to determine if, as the infinite fringe pattern indicates, the major portion of the heat transfer has occurred at a relatively uniform distance from the surface, independent of flow regime.

APPENDICES

APPENDIX A

TEMPERATURE APPROXIMATION A SMALL DISTANCE AWAY FROM THE WALL

In an attempt to explain why turbulent flow heat transfer coefficients are so difficult to measure with a Mach Zehnder interferometer and relatively easy with a differential interferometer, a calculation of the Mach Zehnder fringe shift is made for the same test data that appears in Figure 11 for 45° plate inclination. The calculations show that the number of the Mach Zehnder fringe shifts are about four to six times the number of differential interferometer fringe shifts making interpretation of the Mach Zehnder interferograms potentially more difficult.

In order to determine the temperature a small distance away from the plate an approximation was made that

$$h\,(T_s - T_a) \simeq - k_s \left.\frac{\Delta T}{\Delta y}\right|_s \qquad (1)$$

where $\Delta T = T_s - T_{\Delta y}$ and Δy is the ray separation in the direction normal to the heated surface caused by the first Wollaston prism. In this case $\Delta y = .315 \times 10^{-2}$ feet. Therefore

$$T_{\Delta y} = T_s - \frac{h(T_s - T_a)}{k_s} \Delta y \qquad (2)$$

For a Mach Zehnder interferometer the fringe shift is determined by the equation

$$m = \frac{LG}{R\lambda}\left[\frac{P}{T_{\Delta y}} - \frac{P}{T_a}\right] \qquad (3)$$

assuming constant atmospheric pressure and ideal gas surrounding the plate [57].

From equation (2) and (3) the fringe deflection for the Mach Zehnder can be determined by the differential interferometer for the same conditions. Tabulate below is the instantaneous fringe shift, -m, and the instantaneous temperature, $T_{\Delta y}$, calculated from the instantaneous heat transfer coefficients obtained in Figure 11 for the 45° case.

Table 3. Calculated Data for Figure 1.

$T_{\Delta y}$ for a Period of Five Seconds at a T_x = 282°F								
243.3	232.8	226.0	236.0	234.0	240.5	238.6	251.0	250.2
245.8	238.4	244.0	243.4	234.7	229.8	235.9	241.5	242.1
237.2	226.7	236.0	238.4	238.4	238.4	226.0	230.4	230.4
237.2	247.1	236.0						
Fringe Shift, -m, at Δy from Surface for Corresponding $T_{\Delta y}$.								
28.90	23.37	26.39	27.78	27.50	28.37	28.17	29.78	29.71
29.10	28.10	28.87	28.79	27.63	26.91	27.77	28.50	28.64
27.97	26.48	27.77	28.11	28.10	28.12	26.36	27.03	26.96
27.97	29.29	27.77						
Fringe Shift at the Plate Surface -m = 33.74								

APPENDIX B

Schematic diagrams of heated plate and temperature monitoring system are shown in Figures 13 and 14, respectively.

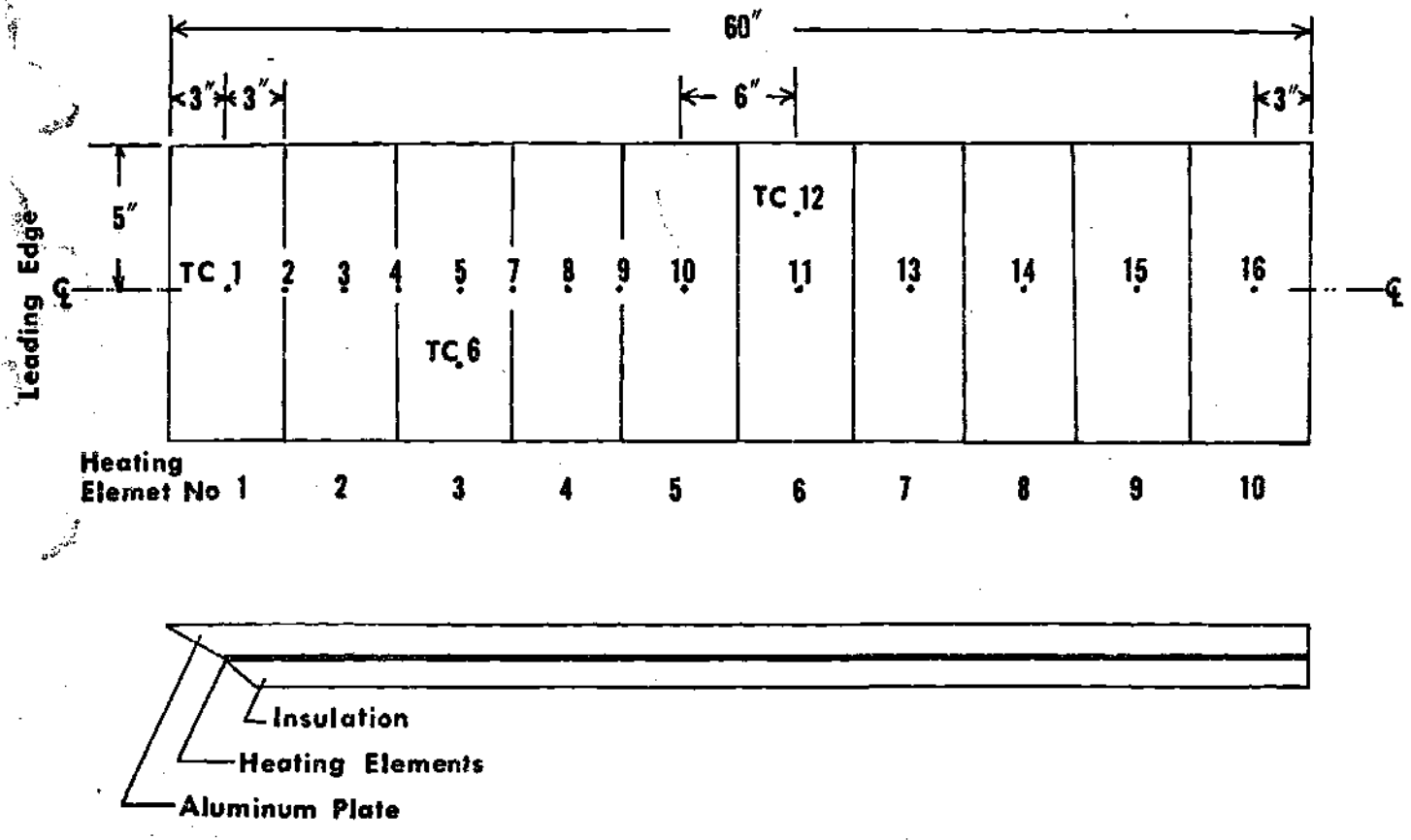

Figure 13. Schematic Diagram of Heated Plate.

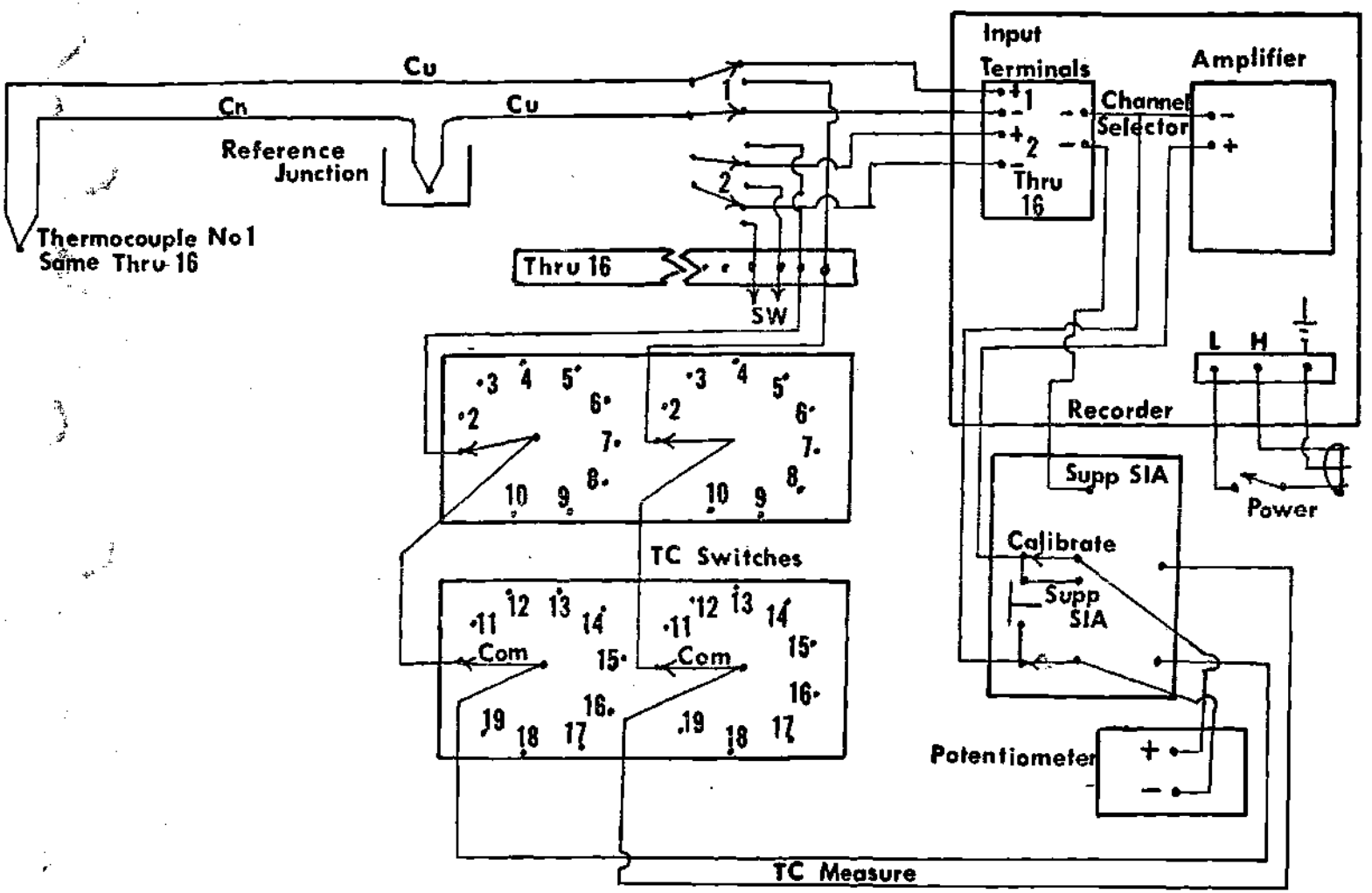

Figure 14. Schematic Diagram of Recorder-Potentiometer Wiring Diagram.

APPENDIX C

OPTIMIZATION OF GRASHOF NUMBER

Since the primary objective of this study was to determine if the differential interferometer could accurately and easily measure the convective heat transfer coefficient, parameters were selected to ensure that a maximum portion of the plate surface area was in the turbulent flow regime. One of the parameters that could be easily varied was the plate surface temperature and the scheme described in this appendix was used to select the plate temperature to insure transition to turbulent flow at a minimum distance from the leading edge of the plate.

The Grashof number is the dimensionless group that is used to determine the type of flow structure in free convection. The Grashof number consists of fluid properties, the length along the surface, and the fluid excess temperature, or

$$Gr_x = \left(\frac{g\beta}{\nu^2}\right)(\Delta T)\ x^3$$

For a given fixed Grashof number corresponding to the critical value, the plate temperature which will yield a minimum value of x will be the one which will maximize the value of the product

$$\frac{g\beta}{\nu^2} \quad (\Delta T).$$

This product is not maximized by simply selecting a maximum for ΔT because the property parameters decrease with increasing ΔT. Therefore, a graphical procedure was used to select a plate temperature to minimize the extent of the laminar area on the plate.

Optimization of Grashof number was accomplished using a T_a = 70°F and

(1) Selecting a ΔT which results in a reference temperature $T_r = T_a + \Delta T/2$.

(2) Determining a Gr/x^3 from the calculated T_r.

(3) Dividing Gr/x^3 into the assumed critical Gr_x.

(4) Plotting the results. A sample calculation: Assume ΔT = 240°F then T_r = 190°F and using reference [32] $Gr/x^3 = 2.02 \times 10^8$ feet^3. The assumed critical $Gr_x = 4 \times 10^8$ for transition. Therefore,

$$\frac{Gr_x}{Gr/x^3} = 1.96 \text{ ft}^3 \text{ or } x = 1.25 \text{ feet}$$

This approach was applied to both the critical Grashof number for turbulent and transition and a plot of x critical as a function of wall temperature was used to determine approximate surface temperature. Figure 15 shows the resulting plots and the fact that a plate surface temperature in the neighborhood of 300°F will result in transition to

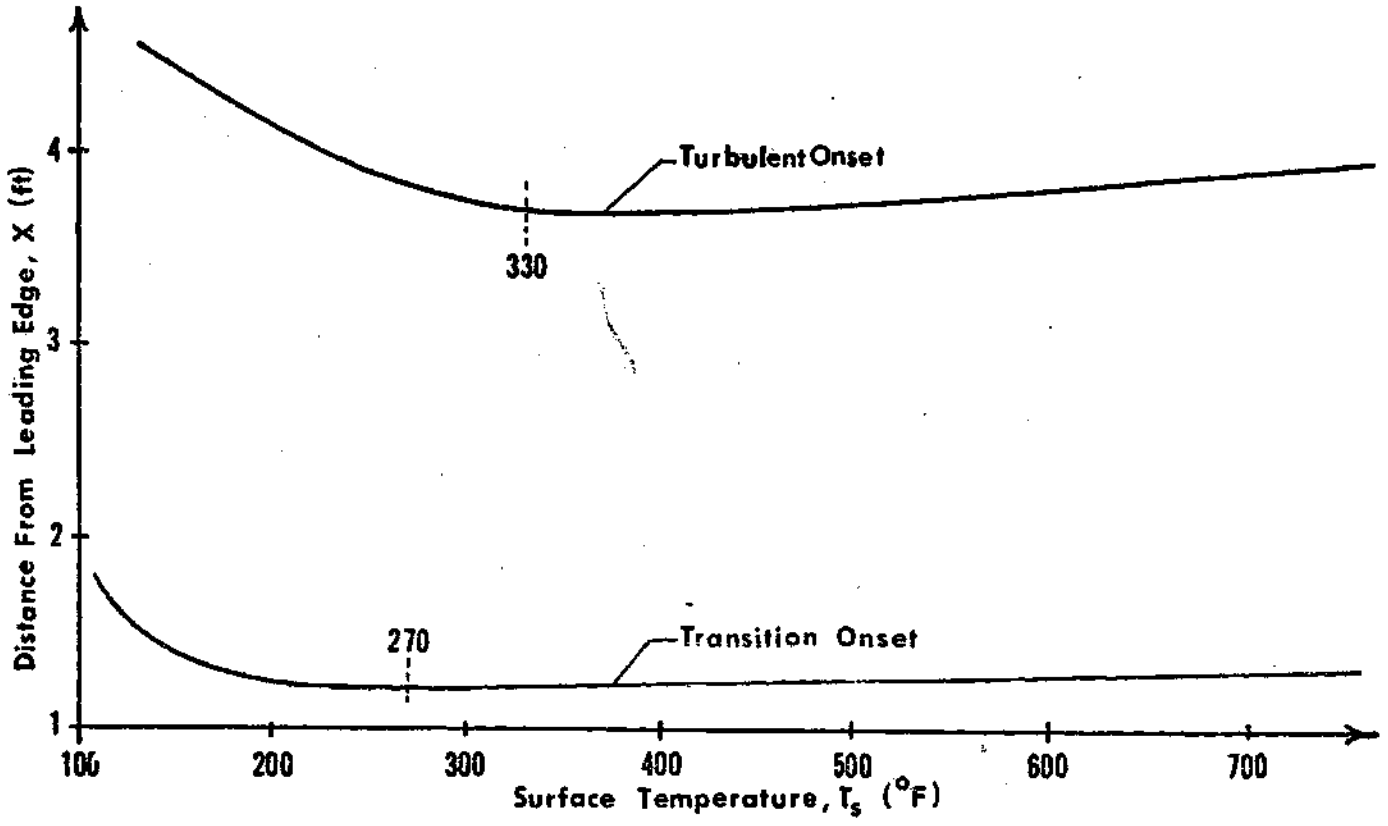

Figure 15. Optimization Curve of Distance from Leading Edge to Onset of Transition and Turbulence as a Function of Surface Temperature.

turbulent flow in a minimum distance from the leading edge of the plate. For this reason the plate temperature was selected to be approximately 280°F, a value which was held constant for test runs.

APPENDIX D

PLATE TEMPERATURE DATA

A complete tabulation of typical temperature data for the plate inclined at 45 degrees and all pertinent results for the other angles are shown in the tables below.

Table 4a. Thermocouple EMF Data for 45° Inclined Plate

TC no.	Time 1 in mV	Time 2 in mV	Time 3 in mV	Time 4 in mV	Time 5 in mV	Air in mV
1	6.120	6.152	6.091	6.082	6.092	1.073
2	6.146	6.177	6.127	6.130	6.150	1.030
3	6.140	6.171	6.100	6.117	6.137	1.085
4	6.129	6.164	6.105	6.100	6.133	1.037
5	6.118	6.165	6.123	6.122	6.132	
6	6.120	6.159	6.116	6.114	6.131	
7	6.162	6.194	6.142	6.123	6.147	
8	6.126	6.173	6.108	6.100	6.118	
9	6.136	6.103	6.110	6.101	6.118	
10	6.118	6.167	6.090	6.078	6.102	
11	not operating properly					
12	6.132	6.184	6.132	6.108	6.137	
13	6.142	6.186	6.108	6.080	6.127	
14	6.150	6.203	6.142	6.105	6.136	
15	6.159	6.193	6.156	6.108	6.133	
16	6.125	6.150	6.115	6.0996	6.1281	
			average			
	6.1427	6.1765	6.1179	6.0996	6.12181	1.0425
			corrected average			
	6.1502	6.1840	6.1254	6.10714	6.1356	1.0425

Table 4b. Average Plate Temperature for All Tests.

Plate	Average T_s	Average high T_s	Average Low T_s	Average T_a
45°	281.7°F	282.5°F	280.7°F	79.9°F
60°	280.0°F	280.9°F	279.1°F	78.6°F
70°	281.7°F	282.5°F	280.8°F	80.2°F
80°	280.8°F	282.1°F	279.9°F	77.0°F

APPENDIX E

PROPERTY VALUES

The following property values were constant for all angles:

$\lambda = 5461$ Å

$\Delta n = .009165$

$G = 3.6257 \times 10^{-3}$ ft^3/lb_m

$L = 10$ in.

$g = 1$ m

$\theta = 0.05236$ Radians

$R = 53.35$ (ft-lbs)/(lb_m-°R)

$Pr = 0.696$

The following properties varied with each angle:

angle	T_r °F	P_{psia}	k_r $(\frac{Btu}{hr\ ft\ ^\circ R})$	k_s $(\frac{Btu}{hr\ ft\ ^\circ R})$	Gr/x^3 $1/ft^3$
45°	180.8	14.00	0.01758	0.01992	1.998×10^8
60°	179.3	14.28	0.01758	0.01990	2.014×10^8
70°	181.0	14.38	0.01761	0.01994	1.975×10^8
80°	178.9	14.27	0.01758	0.01990	2.038×10^8

APPENDIX F

COMPARISON OF NUSSELT NUMBER FOR LAMINAR FLOW REGIME

A comparison between Rich's equation [41] for 45 degree inclination and experimental results is shown in the table below.

Table 5. Laminar Data Comparison.

x ft.	Ra_x	Nu_x	Nu_x(Rich)	% variation
.13281	3.26×10^5	10.827	10.157	6.6
.16146	5.85×10^5	12.451	11.760	5.9
.19010	9.55×10^5	13.882	13.293	3.9
.23698	1.85×10^6	15.662	15.681	-0.1
.24870	2.14×10^6	16.713	16.259	2.8
.25130	2.20×10^6	16.334	16.387	-0.3
.27994	3.05×10^6	17.887	17.769	0.6
.32421	4.74×10^6	20.715	19.836	4.4
.4271	1.08×10^7	27.2	23.958	13.5
.4661	1.41×10^7	24.7	26.036	-4.6
.5599	2.44×10^7	31.1	29.877	4.8
.6523	3.84×10^7	36.5	33.477	9.2 *
.7357	5.54×10^7	40.3	36.682	9.9 *

* In the region of onset of transition.

APPENDIX G

TABULATION OF DATA FOR FIGURE 9

Tabulation of all data plotted in Figure 9.

Table 6. Experimental Data for Figure 9.

45° Plate			60° Plate		
x ft.	Nu_x	$Ra_x \times 10^{-6}$	x ft.	Nu_x	$Ra_x \times 10^{-6}$
.1328	10.827	.3258	.1823	13.74	.8492
.1615	12.451	.5853	.2560	17.09	2.352
.1901	13.822	.9553	.3568	23.82	6.367
.2370	15.662	1.851	.4635	34.60	13.96
.2487	16.713	2.139	.5677	38.78	25.64
.2513	16.334	2.201	.7318	58.92	54.91
.2799	17.887	3.051	.9320	68.59	113.8
.3242	20.715	4.739	1.190	97.21	236.3
.4271	27.200	10.80	1.442	123.1	420.9
.4661	24.700	14.10	1.747	149.0	747.9
.5599	31.000	24.40	2.172	182.2	1427
.6523	36.30	38.40	2.513	201.8	2225
.7357	40.30	55.40	2.859	218.6	3277
.7487	50.30	57.50	3.279	265.5	4940
.8997	68.2	101.0	3.503	294.8	6023
1.022	78.1	148.0	3.721	292.0	7224
1.233	99.0	195.0	4.096	314.0	9635
1.439	122.3	414.0			
1.776	153.6	779.0			
2.072	170.8	1240			
2.391	211.4	1900			
2.658	216.5	2610			
3.013	236.3	3800			
3.307	260.9	5030			
3.587	286.7	6420			
3.793	301.8	7590			

Table 6. (Continued)

70° Plate			80° Plate		
x ft.	Nu_x	$Ra_x \times 10^{-6}$	x ft	Nu_x	$Ra_x \times 10^{-6}$
.1328	8.414	.3219	.1276	8.081	.3012
.1628	12.47	.5926	.1410	9.833	.3976
.1771	14.073	.7635	.1589	11.88	.5691
.2070	17.78	1.111	.1719	13.55	.7362
.2500	20.40	2.148	.1788	14.31	.8101
.4297	27.92	10.91	.2604	23.35	2.505
.6771	49.28	42.62	.3608	33.76	6.663
1.010	89.25	141.6	.4206	29.32	10.55
1.337	106.8	328.7	.5091	33.69	18.72
1.683	137.9	655.8	.7891	59.33	69.69
2.009	153.8	1115	1.242	91.04	271.9
2.428	198.1	1969	1.701	138.3	697.5
2.853	227.2	3192	2.172	185.2	1453
3.201	264.7	4506	2.661	216.0	2674
3.514	273.6	5996	2.990	251.2	3790
3.834	293.8	7744	3.340	249.6	5284
4.111	304.7	9548	3.695	298.0	7158
			4.003	312.6	9096

APPENDIX H

DETERMINATION OF BEST FIT CURVE

Determination of best fit curve for the turbulent data points was computed by using Nu_x values for Ra_x exceeding the critical values for fully turbulent flow listed in Table 2. The remaining data values for Nu_x were divided by $Ra_x^{1/3}$ to obtain a factor c_i. An arithmatical average was calculated. The variance between the arithmatic average and the data points, σ^2, and the standard deviation, σ, were also determined.

The results of these calculations are:

$$\bar{c} = 0.155$$

$$\sigma^2 = 0.3587 \times 10^{-4}$$

$$\sigma = \pm 0.005986$$

with a maximum variation between the curve and all data points of +5.81 percent and -0.9 percent.

APPENDIX I

COMPARISON OF REPEATED DATA

Four data points, two each on the 45° and 80° inclined plate were repeated. The results are as follows:

Table 7. Comparison of Repeated Data.

Angle	Position x ft.	Average m_1	Average m_2	% variation
45°	1.11	5.230	5.202	0.5
45°	1.36	5.518	5.519	0.0
80°	.79	5.032	5.083	1.0
80°	1.24	4.904	4.912	1.6

BIBLIOGRAPHY

1. Aung, W. and Goldstein, R. J., "Temperature Distribution in a Transitional Separated Shear Layer," Heat Transfer, 1970 4th National Heat Transfer Conference, Paris-Versailles, 1970, Vol. 2, F. C. 1.5.

2. Aung, W. and Goldstein, R. J., "Heat Transfer in Turbulent Separated Flow Downstream of a Rearward-Facing Step," Israel Journal of Technology, Vol. 10, 1972, pp. 35-41.

3. Bach, L. H. and Seban, R. A., "On Constant Property Turbulent Boundary Layer with Variable Temperature or Heat Flow at the Wall," ASME, Journal of Heat Transfer, Vol. 87, 1965, pp. 151-156.

4. Bayly, F. J., "An Analysis of Turbulent Free-Convection Heat Transfer," Proceedings of the Institution of Mechanical Engineers, Vol. 169, 1955, pp. 361-368.

5. Black, W. Z. and Carr, W. W., "Application of a Differential Interferometer to the Measurement of Heat Transfer Coefficients," The Review of Scientific Instruments, Vol. 42, 1971, pp. 337-340.

6. Black, W. Z., and Carr. W. W., "A Differential Interferometer and its Application to Heat and Mass Transfer Measurements," ASME Paper No. 72-Ht-12, presented at the ASME-AIChE Transfer Conference, Denver, Colorado, August 1972.

7. Brodowicz, K., "An Analysis of Laminar Free Convection Around Isothermal Vertical Plate," International Journal of Heat and Mass Transfer, Vol. 11, No. 2, 1968, pp. 201-208.

8. Carr, W. W., "The Measurement of Instantaneous, Local Heat Transfer From a Horizontally Vibrating Isothermal Cylinder Using a Differential Interferometer," Ph.D. Thesis in Mechanical Engineering Georgia Institute of Technology, 1973.

9. Catton, I. and Edwards, D. K., "Effect of Side Walls on Natural Convection Between Horizontal Plates Heated From Below," ASME Journal of Heat Transfer, Vol. 89, 1967, pp. 295-299.

10. Cheesewright, R., "Turbulent Natural Convection From a Vertical Plane Surface," ASME Journal of Heat Transfer, Vol. 90, 1968, pp. 1-8.

11. Eckert, E. R. G., "Interferometric Studies of Beginning Turbulence In Free and Forced Convection Boundary Layers on a Heated Plate," Preprints of Papers, Heat Transfer and Fluid Mechanics Institute, 1949, pp. 181-190.

12. Eckert, E. R. G., and Jackson, T. W., "Analysis of Turbulent Free-Convection Boundary Layer," NACA TN 2207, 1950.

13. Eckert, E. R. G. and Soehngen, E., "Interferometric Studies on the Stability and Transition to Turbulence of a Free-Convection Boundary Layer," AF Technical Report 5747, 1948.

14. Fujii, T., "On the Development of a Vortex Street in a Free Convection Boundary Layer," Bulletin of Japan Society of Mechanical Engineers, Vol. 2, 1959, pp. 551-558.

15. Fujii, T., "An Analysis of Turbulent Free Convection Heat Transfer from a Vertical Surface," Bulletin of Japan Society of Mechanical Engineers, Vol. 2, 1959, pp. 559-562.

16. Fujii, T. and Imura, H., "Natural Convection Heat Transfer from a Plate with Arbitrary Inclination," International Journal of Heat and Mass Transfer, Vol. 15, 1972, pp. 755-767.

17. Gebhart, B., "Natural Convection Flow, Instability and Transition," Journal of Heat Transfer, Vol. 91, 1969, pp. 294-309.

18. Gebhart, B., "Transient Natural Convection From Vertical Elements," Journal of Heat Transfer, Vol. 83, 1961, pp. 61-70.

19. Gebhart, B., "Transient Natural Convection From Vertical Elements," Journal of Heat Transfer, Vol. 85, 1963, pp. 10-14.

20. Gebhart, B. and Adams, G. E., "Measurements of Transient Natural Convection on Flat Vertical Surfaces," ASME Journal of Heat Transfer, Vol. 85, 1963, pp. 25-28.

21. Goldstein, R. J. and Chu, T. Y., "Thermal Convection in a Horizontal Layer of Air," Progress in Heat and Mass Transfer, Vol. 2, 1971, pp. 55-75.

22. Goldstein, R. J. and Eckert, E. R. G., "The Steady and Transient Free Convection Boundary Layer on a Uniform Heated Vertical Plate," International Journal of Heat and Mass Transfer, Vol. 1-2, 1960-1961, p. 208.

23. Hama, F. R., Long, J. D. and Hegarty, J. C., "On Transition from Lamiar to Turbulent Flow," Journal of Applied Physics, Vol. 28, 1957, pp. 388-394.

24. Hardwick, N. E. and Levy, E. K., "Study of the Laminar Free Convection Wake Above an Isothermal Vertical Plate," ASME Paper No. 72 WA/HT.

25. Hart, J. E., "Transition to a Wavy Vortex Regime in Convective Flow Between Inclined Plates," Journal of Fluid Mechanics, Vol. 48, 1971, pp. 265-271.

26. Hassan, K. E. and Mohamed, S. A., "Natural Convection From Isothermal Flat Surfaces," International Journal of Heat and Mass Transfer, Vol. 13, 1970, pp. 1873-1885.

27. Holman, J. P., Heat Transfer, 2nd ed., McGraw-Hill Book Company, New York, 1968, pp. 187-209.

28. Holman, J. P., Gartell, H. E. and Soehngen, E. E., "An Interferometric Method of Studying Boundary Layer Oscillations," ASME Journal of Heat Transfer, Vol. 82, 1960, pp. 263-264.

29. Jacob, M., Heat Transfer, Volume 1, John Wiley and Sons, 1964, pp. 577-587.

30. Kato, H., Nishiwaki, N. and Herata, M., "On the Turbulent Heat Transfer by Free Convection From a Vertical Plate," International Journal of Heat and Mass Transfer, Vol. 11, 1968, pp. 1117-1125.

31. Kierkus, W. T., "An Analysis of Laminar Free Convection Flow and Heat Transfer About an Inclined Isothermal Plate," International Journal of Heat and Mass Transfer, Vol. 11, 1968, pp. 241-253.

32. Kreith, F., Principles of Heat Transfer, 2nd ed. International Textbook Company, Scranton, Pennsylvania, 1958.

33. Kutateladze, S. S., Kirdyashkin, A. G., and Ivakin, V. P., "Turbulent Natural Convection on a Vertical Plate and in a Vertical Layer," International Journal of Heat and Mass Transfer, Vol. 15, 1972, pp. 193-202.

34. Lemlick, R. and Vardi, J., "Steady Free Convection to a Flat Plate with Uniform Surface Heat Flux and Nonuniform Acceleration," ASME Journal of Heat Transfer, Vol. 86, 1964, p. 562.

35. Lloyd, J. R., Sparrow, E. M., and Eckert, E. R. G., "Laminar Transition and Turbulent Natural Convection Adjacent to Inclined and Vertical Surfaces," International Journal of Heat and Mass Transfer, Vol. 15, 1972, pp. 457-472.

36. Lloyd, J. R., and Sparrow, E. M., "On the Instability of Natural Convection Flow on Inclined Plates," Journal of Fluid Mechanics, Vol. 42, 1970, pp. 465-470.

37. Lock, C. S. H. and Trotter, F. J., "Observations on Surface of Turbulent Free-Convection Boundary Layer," International Journal of Heat and Mass Transfer, Vol. 11, 1968, pp. 1225-1232.

38. Mordchelles-Regnier, G. and Kaplan, C., "Visualization of Natural Convection on a Plane Wall and in Vertical Gap by Differential Interferometer, Transition and Turbulent Regimes," Proceedings of the 1963 Heat Transfer and Fluid Mechanics Institute, 1963, p. 105.

39. McAdams, W. H., Heat Transmission, 3rd ed., McGraw-Hill Book Company, Inc., New York, 1954, pp. 165-183.

40. McKie, W. T., "Laminar Free Convection about Inclined Isothermal Surfaces for Fluids with Temperature Dependent Properties," Ph.D. Thesis in Mechanical Engineering, Georgia Institute of Technology, 1968.

41. Rich, B. R., "An Investigation of Heat Transfer From an Inclined Flat Plate in Free Convection," Transactions of ASME, Vol. 75, 1953, p. 489.

42. Sernas, V. and Fletcher, L. S., "A Schlieren Interferometer Method for Heat Transfer Studies," ASME Journal of Heat Transfer, Vol. 92, 1970, p. 202.

43. Siegel, R., "Transient Free Convection From a Vertical Flat Plate," Transactions of ASME, Vol. 80, 1958, p. 347.

44. Sparrow, E. M. and Gregg, J. L., "Laminar Free Convection from a Vertical Plate with Uniform Surface Heat Flux," Transactions of ASME, Vol. 78, 1956, p. 435.

45. Sparrow, E. M. and Gregg, J. L., "Similar Solutions for Free Convection From a Nonisothermal Vertical Plate," Transactions of ASME, Vol. 80, 1958, p. 379.

46. Sparrow, E. M. and Husar, R. B., "Longitudinal Vortices in Natural Convection Flow on Inclined Plates," Journal of Fluid Mechanics, Vol. 37, 1969, p. 251.

47. Szenczyk, A. A., "Stability and Transition of the Free Convection Boundary Layer Along a Flat Plate," International Journal of Heat and Mass Transfer, Vol. 5, 1962, p. 903.

48. Tritton, D. J., "Turbulent Free Convection Above a Heated Plate Inclined at a Small Angle to the Horizontal," Journal of Fluid Mechanics, Vol. 16, 1963, p. 282.

49. Tritton, D. J., "Transition to Turbulence in the Free Convection Boundary Layers on an Inclined Heated Plate," Journal of Fluid Mechanics, Vol. 16, 1963, p. 417.

50. Van Sant, J. H., "Temperature Variation on the Surface of a Strip-Heated Flat Plate," ASME Journal of Heat Transfer, Vol. 89, 1967, p. 372.

51. Vliet, C. G., "Natubal Convection Local Heat Transfer on Constant Heat Flux Inclined Surfaces," ASME Paper No. 69-HT-C.

52. Vliet, C. G., and Liu, C. K., "An Experimental Study of Turbulent Natural Convection Boundary Layers," ASME Journal of Heat Transfer, Vol. 91, 1969, p. 577.

53. Warner, C. Y. and Arpaci, V. S., "An Experimental Investigation of Turbulent Natural Convection in Air at Low Pressure Along a Vertical Heated Flat Plate," International Journal of Heat and Mass Transfer, Vol. 11, p. 397.

54. Yang, K. T. and Jerger, E. W., "First-Order Perturbations of Laminar Free Convection Boundary Layer on a Vertical Plate," Journal of Heat Transfer, Vol. 68, 1964, p. 107.

55. Yung, S. C. and Oetting, R. B., "Free Convection Heat Transfer from an Inclined Heated Plate in Air," ASME Journal of Heat Transfer, Vol. 68 , 1969, p. 192.

56. Weast, R. C., Editor, Handbook of Chemistry and Physics, 50th ed., the Chemical Rubber Company, 1964-1970.

57. ME 315/317, "Notes on the Use of Optical Methods in Heat and Mass Transfer," School of Mechanical Engineering, Georgia Institute of Technology, pp. 2563-4-11.